Joint User Pairing and Resource Allocation in a SWIPT-Enabled Cooperative NOMA System

Mengru Wu [ID], *Student Member, IEEE*, Qingyang Song [ID], *Senior Member, IEEE*,
Lei Guo [ID], *Member, IEEE*, and Abbas Jamalipour [ID], *Fellow, IEEE*

Abstract—This paper studies a novel design of user pairing and resource allocation in a simultaneous wireless information and power transfer (SWIPT)-enabled cooperative non-orthogonal multiple access (NOMA) system with coexisting power-splitting (PS) and time-switching (TS) users. In this system, near NOMA users (NUs) that are close to a source can assist the communications between the source and far NOMA users (FUs) using the energy harvested by either PS or TS strategy. The design aims to maximize the sum-rate of the system by optimizing user pairing and power allocation between NUs and FUs as well as performing PS and TS control at NUs, while guaranteeing the target data rates and the minimum harvested energy requirements of users. Since the joint design is formulated as a non-convex mixed-integer non-linear programming (MINLP) problem that is challenging to tackle, we propose a two-step user pairing and resource allocation algorithm. Specifically, we decouple the original problem into an inner resource allocation problem and an outer user pairing problem. For the inner problem, we propose successive convex approximation (SCA) and block coordinate descent (BCD)-based algorithms to perform power allocation as well as PS and TS control iteratively, with the algorithms' convergence being theoretically proved. By exploiting the characteristics of the outer problem of user pairing, this problem is well tackled by the Hungarian algorithm. Simulation results demonstrate the proposed joint design yields better performance gains than the existing schemes.

Index Terms—Simultaneous wireless information and power transfer (SWIPT), non-orthogonal multiple access (NOMA), cooperative communications, resource allocation.

I. INTRODUCTION

THE fifth-generation (5G) communication networks are expected to support an ever-increasing number of wireless devices, such as Internet-of-Things (IoT) devices. However, the limited resources of wireless networks make it difficult to provide the massive connectivity of those devices. In this context, non-orthogonal multiple access (NOMA) has drawn extensive attention, since it can offer significant improvements in connectivity and spectral efficiency in comparison to orthogonal multiple access (OMA) [1]. The basic principle of NOMA is to allow multiple users with different channel conditions to be served in the same resource block by power-domain multiplexing [2]. That is, NOMA controls transmit signals at different power levels and removes the co-channel interferences caused by the use of non-orthogonal resources via successive interference cancellation (SIC) [3]. Motivated by the benefits of NOMA, many efforts have been paid to integrate NOMA into wireless networks. In [4], the authors discussed the application of NOMA in cooperative communications. Besides, NOMA has also been proposed to be incorporated into other technologies such as cognitive radio communications [5], [6], mobile edge computing [7], and wireless powered communications [8].

In addition to connectivity and spectral efficiency improvements, it is also significant to prolong the lifetime of energy-constrained networks, e.g., IoT networks and wireless sensor networks (WSNs). Simultaneous wireless information and power transfer (SWIPT) has emerged as a promising technology to alleviate energy limitation for battery-powered devices in the next generation of wireless communications and beyond [9]. The key idea of SWIPT is exploiting the same emitted electromagnetic wave to deliver both energy and information, which is beneficial to explore energy-efficient networks [10]. However, in reality, it is challenging to extract energy and information by the same circuit module due to hardware limitations [11]. To deal with this difficulty, some practical SWIPT receiver architectures have been proposed, among which power-splitting (PS) and time-switching (TS) receivers are better-known and realistic. In particular, a PS receiver can split its received signals into an energy harvesting (EH) part and an information decoding (ID) part, which are respectively sent to EH and ID circuits [12], [13]. A TS receiver can switch its operation between ID and EH modes in orthogonal time slots [14].

A. Related Works

Recently, the integration of NOMA and SWIPT into cooperative communication networks, termed as cooperative SWIPT NOMA systems or SWIPT-enabled cooperative NOMA

systems, has emerged as a new paradigm to improve system performance and enhance network coverage. In SWIPT-enabled cooperative NOMA systems,[1] a source serves users by employing NOMA, and strong users with good channel conditions can spend the energy harvested by SWIPT assisting the communications between the source and weak users with poor channel conditions. The outage performance of SWIPT-enabled cooperative NOMA systems was investigated in [15]–[18]. Specifically, the authors in [15] analyzed the impacts of different user pairing schemes between weak users and strong users on the outage performance of SWIPT-enabled cooperative NOMA systems under fixed power allocation coefficients. To enhance the outage performance of near users, the authors in [16] jointly designed power allocation coefficients and PS factors in cooperative SWIPT NOMA systems. The authors in [17] studied the outage probability and ergodic rate of a SWIPT-enabled NOMA system with full-duplex (FD) relaying, in which a near NOMA user (NU) is capable of assisting a far NOMA user (FU) using the energy harvested by a TS strategy. The authors in [18] proposed a best-near best-far (BNBF) user selection scheme for SWIPT-enabled cooperative NOMA systems, in which near users power their relaying operations using the PS strategy. They further derived the approximate expressions of outage probability for three relaying protocols, i.e., decode-and-forward (DF), amplify-and-forward (AF), and hybrid DF/AF protocols.

Besides, resource allocation schemes have been studied in [19]–[23] for improving the system performance of cooperative SWIPT NOMA networks and enhancing resource utilization efficiency. In [19], the authors considered a near user with a strong channel condition acts as an energy-harvesting relay to help a far user with a poor channel condition based on the PS strategy. Their objective is to maximize the data rate of the near user while guaranteeing the quality-of-service (QoS) requirement of the far user in multiple-input single-output and single-input single-output cases. [20] and [21] further studied a three-node cooperative SWIPT NOMA system, in which a NU helps the information transmission from a source to a FU and the channel state information (CSI) between the source and two NOMA users is uncertain. They jointly designed robust transmit beamforming and PS control for improving system performance. The authors in [22] studied a system where a nearby user assists the information transmission between an access point and a far-end user. Besides, transmit power minimization problems were studied via a joint optimization of transmit beamforming vectors at the access point and PS control at the nearby user. In [23], the authors considered a cell-center user acts as an FD relay to help a cell-edge user using the energy harvested by the PS receiver, and energy efficiency maximization problems were studied in this system.

B. Motivations and Contributions

In the existing works mentioned above [15]–[23], PS and TS receiver architectures were separately investigated in various

cooperative SWIPT NOMA systems to prolong the lifetime of NUs. To be specific, the existing works mainly considered NUs employ either only PS receivers or TS receivers to power their relaying operations. Nevertheless, in practical systems (e.g., IoT networks and WSNs), wireless devices may be produced by different manufactures with different receiver architectures, and some of these devices are inevitably deployed in the same wireless communication network. We note that general SWIPT networks, in which some users employ PS receivers and the others adopt TS receivers, were studied in [24].[2] To our best knowledge, no prior work investigates general cooperative SWIPT NOMA networks involving various users with different types of SWIPT receivers. Besides, [19]–[23] mainly focused on designing efficient resource allocation schemes for a simple three-node scenario consisting of a source, a NU equipped with the PS receiver architecture, and a FU without considering user pairing. But realistic networks are rather complex due to the existence of many NUs and FUs. In this regard, investigating the pairing strategy between multiple NUs and FUs to form cooperative pairs is of significance for improving the system performance of cooperative SWIPT NOMA systems.

Motivated by the above discussions, we propose a novel design of user pairing and resource allocation for a general cooperative SWIPT NOMA system. In the considered system, a source serves multiple NUs and FUs. Some NUs are equipped with PS receiver architectures and the others are endowed with TS receiver architectures. These two kinds of users are respectively termed as power-splitting users (PSUs) and time-switching users (TSUs). We consider a NU and a FU are selected to form a cooperative NOMA pair, in which the source serves the two users via NOMA and the NU acts as an energy-harvesting relay to satisfy the QoS requirement of the FU. Besides, the conventional time division multiple access (TDMA) technology is used to serve different user pairs. The key goal of this paper is to jointly optimize user pairing, power allocation, PS and TS control to maximize the sum-rate of the system while satisfying the minimum data rates and harvested energy requirements of users. The main contributions of this paper are summarized as follows:

- We investigate a general downlink cooperative SWIPT NOMA system, which consists of multiple coexisting PSUs and TSUs. A novel optimization problem that jointly determines user pairing between NUs (i.e. PSUs and TSUs) and FUs, allocates power to NUs and FUs, as well as performs PS and TS control at NUs is formulated to maximize the sum-rate of all users. Due to the presence of coupled variables and the intra-interference of a NOMA pair, the formulated problem is a non-convex mixed-integer non-linear programming (MINLP) problem that is intricate challenging to solve.

- We develop a two-step user pairing and resource allocation algorithm to solve the formulated problem. Specifically, we decompose the problem into an inner resource allocation

---

[1]In existing works, SWIPT-enabled cooperative NOMA systems can be divided into two kinds in terms of the types of relays, i.e., user-aided and dedicated relay-assisted systems, and this paper focuses on the first kind.

[2]Compared with [24], this work employs cooperative communications and NOMA to improve system performance, which makes resource allocation and user pairing problems more intractable.
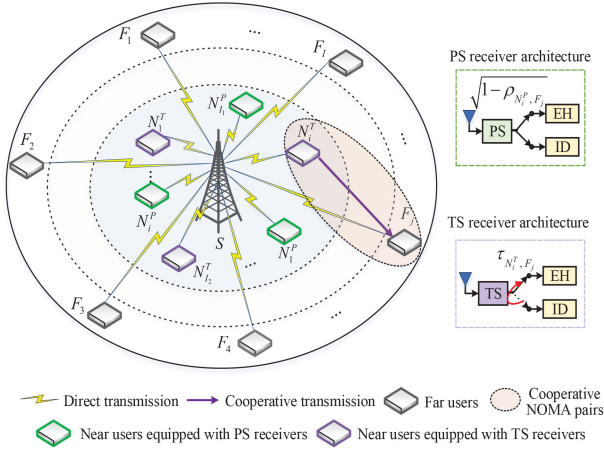
Fig. 1.   Illustration of a general cooperative SWIPT NOMA system.

problem and an outer user pairing problem. For the inner problem, the block coordinate descent (BCD) method is employed by partitioning the resource allocation optimization variables into two blocks: the power allocation block and the PS and TS control block. For the non-convex optimization of each block, based on a series of transformations, successive convex approximation (SCA) is employed to convert the non-convex problems into convex. The outer problem of user pairing is cast into a maximum weighted bipartite matching (MWBM) problem and then solved by the Hungarian algorithm.

- The proposed joint user pairing and resource allocation (JUPRA) scheme is evaluated and compared with the existing baseline schemes through simulations. The results demonstrate that the proposed scheme outperforms the baseline schemes and enhances the network sum-rate. Meanwhile, the convergence of the SCA and the BCD-based algorithms are respectively evaluated.

The rest of the paper is organized as follows. Section II presents the system model of the general cooperative SWIPT NOMA system and the formulated sum-rate maximization problem. In Section III, we propose the joint design of user pairing and resource allocation. In Section IV, simulation results are presented and analyzed. Finally, we conclude this paper in Section V.

II. SYSTEM MODEL AND PROBLEM FORMULATION

A. System Model

We consider a downlink communication system, in which a source S serves two groups of users $\mathcal{N} = \{N_1, \ldots, N_i, \ldots, N_I\}$ and $\mathcal{F} = \{F_1, \ldots, F_j, \ldots, F_I\}$. As shown in Fig. 1, the users in $\mathcal{N}$ are close to the source and distributed within a disc, and the users in $\mathcal{F}$ are far away from the source and distributed within a ring. In this system, S is located at the origin of both the disc and the ring, and the users in $\mathcal{N}$ and $\mathcal{F}$ are respectively referred to as NUs and FUs. Similar to [25], we consider the number of the NUs is equal to that of the FUs. To satisfy the quality-of-service (QoS) requirement of a FU, a NU acts as a friendly relay to assist

the information transmission from S to the FU. In this context, the NU and the FU form a cooperative user pair and can be served by S via NOMA. The conventional TDMA technology is used to serve different cooperative user pairs. We assume that the total time T is equally divided into I slots and the duration of each slot $t = \frac{T}{I}$ is the transmission time of a cooperative NOMA pair. Besides, as the assumption in [15], [26]–[28], all channel gains are considered to be known by S to explore a performance upper bound.

To prolong the lifetime of this network, we consider that the NUs employ SWIPT receiver architectures to power their relaying operations. That is, the NUs are capable of harvesting energy from the signals transmitted by S via SWIPT. Besides, we consider a practical and general scenario, i.e., some NUs are equipped with PS receiver architectures, and the others are endowed with TS receiver architectures. In this context, the NUs can be further divided into the group of PSUs $\mathcal{N}^P = \{N_1^P, \ldots, N_i^P, \ldots, N_{I_1}^P\}$ and the group of TSUs $\mathcal{N}^T = \{N_1^T, \ldots, N_i^T, \ldots, N_{I_2}^T\}$, where $I_1 + I_2 = I$, $\mathcal{N}^P \cup \mathcal{N}^T = \mathcal{N}$, and $\mathcal{N}^P \cap \mathcal{N}^T = \mathbf{0}$, where $\mathbf{0}$ denotes the null set. We assume each FU is scheduled to pair with one NU and vice versa. To specify the user pairing relationships between the NUs and the FUs, we define two-dimensional paring matrices $\boldsymbol{\Psi_1} \in \mathbb{R}^{I_1 \times I}$ and $\boldsymbol{\Psi_2} \in \mathbb{R}^{I_2 \times I}$. Each element in these two matrices is a binary integer variable. Specifically, $\Psi_{N_i^P, F_j} = 1$ ($\forall \Psi_{N_i^P, F_j} \in \boldsymbol{\Psi_1}$) means a PSU N_i^P ($\forall N_i^P \in \mathcal{N}^P$) is selected to pair with a FU F_j ($\forall F_j \in \mathcal{F}$); otherwise $\Psi_{N_i^P, F_j} = 0$. Similarly, if $\Psi_{N_i^T, F_j} = 1$ ($\forall \Psi_{N_i^T, F_j} \in \boldsymbol{\Psi_2}$), it means a TSU N_i^T ($\forall N_i^T \in \mathcal{N}^T$) is selected to pair with a FU F_j ($\forall F_j \in \mathcal{F}$); otherwise $\Psi_{N_i^T, F_j} = 0$. For ease of reference, some key notations used in this paper are summarized in Table I.

B. Achievable Rate Analysis for a Matched PSU-FU Pair

For a matched PSU and FU pair, i.e., a PSU N_i^P ($\forall N_i^P \in \mathcal{N}^P$) is selected to pair with a FU F_j ($\forall F_j \in \mathcal{F}$) and $\Psi_{N_i^P, F_j} = 1$, the transmission model of the pair consists of two phases. During the direct transmission phase, S transmits a superimposed signal $x = \sqrt{\alpha_{N_i^P, F_j} P_S} x_{N_i^P} + \sqrt{(1 - \alpha_{N_i^P, F_j}) P_S} x_{F_j}$ both to N_i^P and F_j, where $x_{N_i^P}$ and x_{F_j} respectively denote the intended signals of N_i^P and F_j, P_S is the transmit power of S, $\alpha_{N_i^P, F_j} P_S$ and $(1 - \alpha_{N_i^P, F_j}) P_S$ are the transmit powers allocated to N_i^P and F_j, respectively. Besides, N_i^P employs the PS strategy for EH and ID. Specifically, it can split the received signal into two streams, i.e., one stream with power ratio $\rho_{N_i^P, F_j}$ is used for ID and the other stream with power ratio $(1 - \rho_{N_i^P, F_j})$ is used for EH. Therefore, the received signals for ID at F_j and N_i^P and the energy harvested by N_i^P can be respectively given by [15]

$$y_{F_j}^{(1)} = h_{S,F_j} \left[\sqrt{\alpha_{N_i^P, F_j} P_S} x_{N_i^P} \right.$$
$$\left. + \sqrt{(1 - \alpha_{N_i^P, F_j}) P_S} x_{F_j} \right] + n_{F_j}, \quad (1)$$

$$y_{N_i^P}^{(1)} = \sqrt{\rho_{N_i^P, F_j}} h_{S,N_i^P} \left[\sqrt{\alpha_{N_i^P, F_j} P_S} x_{N_i^P} \right.$$
$$\left. + \sqrt{(1 - \alpha_{N_i^P, F_j}) P_S} x_{F_j} \right] + n_{N_i^P}, \quad (2)$$

Notation	Description
$\mathcal{N}$	Set of all NUs.
$\mathcal{F}$	Set of all FUs.
I	Number of NUs or FUs.
$\mathcal{N}^P$	Set of NUs equipped with PS receivers.
$\mathcal{N}^T$	Set of NUs endowed with TS receivers.
I_1	Number of PSUs.
I_2	Number of TSUs.
t	Transmission time of a cooperative NOMA pair.
$\Psi_{N_i^P, F_j}$	User pairing indicator between PSU N_i^P and FU F_j.
$\Psi_{N_i^T, F_j}$	User pairing indicator between TSU N_i^T and FU F_j.
x_{F_j}	Intended message of FU F_j.
$x_{N_i^P}$	Intended message of PSU N_i^P.
$x_{N_i^T}$	Intended message of TSU N_i^T.
h_{S, F_j}	Channel coefficient from S to FU F_j.
h_{S, N_i^P}	Channel coefficient from S to PSU N_i^P.
h_{S, N_i^T}	Channel coefficient from S to TSU N_i^T.
$h_{N_i^P, F_j}$	Channel coefficient from PSU N_i^P to FU F_j.
$h_{N_i^T, F_j}$	Channel coefficient from TSU N_i^T to FU F_j.
P_S	Transmit power of S.
σ^2	Additive noise power.
$\alpha_{N_i^P, F_j}$	Power allocation coefficient for PSU N_i^P.
$\alpha_{N_i^T, F_j}$	Power allocation coefficient for TSU N_i^T.
η	Energy conversion efficiency.
$\rho_{N_i^P, F_j}$	PS ratio for performing ID at PSU N_i^P.
$\tau_{N_i^T, F_j}$	TS factor for performing EH at TSU N_i^T.
$\tilde{\tau}_{N_i^T, F_j}$	TS factor for information transmission at TSU N_i^T.

$$E_{N_i^P} = \frac{t}{2}\eta(1 - \rho_{N_i^P, F_j})P_S|h_{S, N_i^P}|^2, \qquad (3)$$

where h_{S, F_j} and h_{S, N_i^P} are respectively the channel coefficients from S to F_j and N_i^P, n_{F_j} and $n_{N_i^P}$ denote the additive white Gaussian noise (AWGN) with zero mean and variance σ^2 [29], [30]. Besides, $0 \leq \eta \leq 1$ is the constant energy conversion efficiency. In (3), $\frac{t}{2}$ is caused by the assumption that the two phases have the same periods, which is same to [15] and [21]. Dynamic time allocation for the two phases may improve system performance, but the consideration of this issue is beyond the scope of the paper.

Following the principle of NOMA, F_j only decodes x_{F_j} by treating $x_{N_i^P}$ as noise, and SIC is employed by N_i^P to combat the negative effect of the inter-user interference caused by F_j. Specifically, N_i^P first decodes x_{F_j} and then subtracts this component from its received signal to decode its information $x_{N_i^P}$. Accordingly, the signal-to-interference-plus-noise ratio (SINR) for F_j to decode x_{F_j} and the SINR for N_i^P to decode x_{F_j} are respectively written as

$$\gamma_{F_j, x_{F_j}}^{(1)} = \frac{(1 - \alpha_{N_i^P, F_j})|h_{S, F_j}|^2}{\alpha_{N_i^P, F_j}|h_{S, F_j}|^2 + \frac{\sigma^2}{P_S}}, \qquad (4)$$

$$\gamma_{N_i^P, x_{F_j}}^{(1)} = \frac{\rho_{N_i^P, F_j}(1 - \alpha_{N_i^P, F_j})|h_{S, N_i^P}|^2}{\rho_{N_i^P, F_j}\alpha_{N_i^P, F_j}|h_{S, N_i^P}|^2 + \frac{\sigma^2}{P_S}}, \qquad (5)$$

After successfully decoding the information of F_j, N_i^P can subtract the message x_{F_j} from its reception and decode its information $x_{N_i^P}$. Consequently, when N_i^P is paired with F_j, the signal-to-noise ratio (SNR) for N_i^P to decode $x_{N_i^P}$ and the corresponding achievable rate can be respectively written as

$$\gamma_{N_i^P, x_{N_i^P}}^{(1)} = \frac{\rho_{N_i^P, F_j}\alpha_{N_i^P, F_j}|h_{S, N_i^P}|^2}{\frac{\sigma^2}{P_S}}. \qquad (6)$$

$$R_{N_i^P, F_j} = \frac{t}{2}\log_2\left(1 + \gamma_{N_i^P, x_{N_i^P}}^{(1)}\right). \qquad (7)$$

In the cooperative transmission phase, N_i^P can act as a DF relay that forwards x_{F_j} to F_j utilizing the harvested energy $E_{N_i^P}$. The received signal at F_j in the cooperative phase can be expressed as

$$y_{F_j}^{(2)} = h_{N_i^P, F_j}\sqrt{P_{N_i^P}^r}\, x_{F_j} + n_{F_j}, \qquad (8)$$

where $P_{N_i^P}^r$ is the transmit power of N_i^P for relaying information, and $h_{N_i^P, F_j}$ represents the channel coefficient from N_i^P to F_j. We assume the energy harvested by N_i^P is only used for information transmission, while the energy consumed for maintaining transceiver circuits and signal processing is not considered in this paper. As a result, $P_{N_i^P}^r = E_{N_i^P}/\frac{t}{2} = \eta(1 - \rho_{N_i^P, F_j})P_S|h_{S, N_i^P}|^2$ can be obtained. Then, the SNR for F_j to detect x_{F_j} is given by

$$\gamma_{F_j, x_{F_j}}^{(2)} = \frac{\eta(1 - \rho_{N_i^P, F_j})|h_{S, N_i^P}|^2|h_{N_i^P, F_j}|^2}{\frac{\sigma^2}{P_S}}. \qquad (9)$$

In fact, F_j receives two copies of x_{F_j} through two different links, i.e., one comes from S and the other one comes from N_i^P. Based on the maximal-ratio combining (MRC) technique, F_j combines the SINR of the direct transmission phase in (4) and the SNR of the cooperative transmission phase in (9). Based on the above analysis and the results in [25], the achievable rate of F_j from the cooperative diversity of S and N_i^P is expressed as

$$R_{F_j, N_i^P} = \frac{t}{2}\min\left\{\log_2\left(1 + \gamma_{N_i^P, x_{F_j}}^{(1)}\right),\right.$$
$$\left.\log_2\left(1 + \gamma_{F_j, x_{F_j}}^{(1)} + \gamma_{F_j, x_{F_j}}^{(2)}\right)\right\}, \qquad (10)$$

where the minimum operation is caused by the DF strategy.

C. Achievable Rate Analysis for a Matched TSU-FU Pair

Then, we analyze the case of a matched TSU and FU pair, i.e., a TSU N_i^T ($\forall N_i^T \in \mathcal{N}^T$) is selected to pair with a FU F_j ($\forall F_j \in \mathcal{F}$) and $\Psi_{N_i^T, F_j} = 1$. Due to the time switching feature of TSUs, the achievable rate and harvested energy of a matched TSU-FU pair are different from that of a matched PSU-FU pair. During the first phase, S transmits a superimposed signal $x' = \sqrt{\alpha_{N_i^T, F_j}P_S}x_{N_i^T} + \sqrt{(1 - \alpha_{N_i^T, F_j})P_S}x_{F_j}$ both to N_i^T and F_j, where $x_{N_i^T}$ denotes the intended signal of N_i^T, $\alpha_{N_i^T, F_j}P_S$ and $(1 - \alpha_{N_i^T, F_j})P_S$ are the transmit powers allocated to N_i^T and F_j, respectively. For N_i^T, it can employ

the TS strategy to perform EH and ID. That is, N_i^T spends $\tau_{N_i^T, F_j}$ $(0 \leq \tau_{N_i^T, F_j} \leq t)$ harvesting energy from the signal sent by S. The fraction $\widetilde{\tau}_{N_i^T, F_j}$ $(0 \leq \widetilde{\tau}_{N_i^T, F_j} \leq t)$ is used for the information transmission from S to N_i^T. That is, $\tau_{N_i^T, F_j}$ and $\widetilde{\tau}_{N_i^T, F_j}$ are TS factors at N_i^T. Then, the SINR for F_j to decode x_{F_j}, the SINR for N_i^T to decode x_{F_j}, and the energy harvested by N_i^T are respectively written as

$$\gamma_{F_j, x_{F_j}}^{(1)'} = \frac{(1 - \alpha_{N_i^T, F_j})|h_{S, F_j}|^2}{\alpha_{N_i^T, F_j}|h_{S, F_j}|^2 + \frac{\sigma^2}{P_S}}, \tag{11}$$

$$\gamma_{N_i^T, x_{F_j}}^{(1)} = \frac{(1 - \alpha_{N_i^T, F_j})|h_{S, N_i^T}|^2}{\alpha_{N_i^T, F_j}|h_{S, N_i^T}|^2 + \frac{\sigma^2}{P_S}}, \tag{12}$$

$$E_{N_i^T} = \tau_{N_i^T, F_j} \eta P_S |h_{S, N_i^T}|^2, \tag{13}$$

where h_{S, N_i^T} is the channel coefficient from S to N_i^T. After the information transmitted to F_j is successfully decoded by N_i^T, the SNR for N_i^T to decode $x_{N_i^T}$ and the corresponding achievable rate can be respectively given by

$$\gamma_{N_i^T, x_{N_i^T}}^{(1)} = \frac{\alpha_{N_i^T, F_j}|h_{S, N_i^T}|^2}{\frac{\sigma^2}{P_S}}, \tag{14}$$

$$R_{N_i^T, F_j} = \widetilde{\tau}_{N_i^T, F_j} \log_2 \left(1 + \gamma_{N_i^T, x_{N_i^T}}^{(1)}\right). \tag{15}$$

In the second phase with duration $\widetilde{\tau}_{N_i^T, F_j}$, N_i^T adopts the DF strategy and forwards x_{F_j} to F_j with the transmit power $P_{N_i^T}^r$. Since the harvested energy is only used for relaying information, we have $P_{N_i^T}^r = E_{N_i^T}/\widetilde{\tau}_{N_i^T, F_j} = \tau_{N_i^T, F_j} \eta P_S |h_{S, N_i^T}|^2/\widetilde{\tau}_{N_i^T, F_j}$. Let $h_{N_i^T, F_i}$ represent the channel coefficient from N_j^T to F_j. The SNR for F_j to decode x_{F_j} can be expressed as

$$\gamma_{F_j, x_{F_j}}^{(2)'} = \frac{\tau_{N_i^T, F_j} \eta |h_{S, N_i^T}|^2 |h_{N_i^T, F_j}|^2}{\widetilde{\tau}_{N_i^T, F_j} \frac{\sigma^2}{P_S}}, \tag{16}$$

At the end of the second phase, F_j decodes x_{F_j} based on the signals received from S and N_i^T using MRC. The achievable rate of F_j when it is paired with N_i^T can be given by

$$R_{F_j, N_i^T} = \widetilde{\tau}_{N_i^T, F_j} \min \left\{ \log_2 \left(1 + \gamma_{N_i^T, x_{F_j}}^{(1)}\right), \right.$$
$$\left. \log_2 \left(1 + \gamma_{F_j, x_{F_j}}^{(1)'} + \gamma_{F_j, x_{F_j}}^{(2)'}\right) \right\}. \tag{17}$$

D. Problem Formulation

This paper aims to maximize the network sum-rate by jointly optimizing user paring between the NUs and the FUs, power allocation at S, as well as PS and TS control. Accordingly, the problem is mathematically formulated as

$$\mathcal{OP}: \max_{\substack{\Psi, \alpha_1, \\ \alpha_2, \rho, \tau, \widetilde{\tau}}} \sum_{F_j \in \mathcal{F}} \sum_{N_i^P \in \mathcal{N}^P} \Psi_{N_i^P, F_j} (R_{N_i^P, F_j} + R_{F_j, N_i^P})$$

$$+ \sum_{F_j \in \mathcal{F}} \sum_{N_i^T \in \mathcal{N}^T} \Psi_{N_i^T, F_j} (R_{N_i^T, F_j} + R_{F_j, N_i^T}) \tag{18a}$$

s.t. $R_{N_i^P, F_j} \geq R_{th}^{N_i}, \ R_{F_j, N_i^P} \geq R_{th}^{F_j}, \ \text{if } \Psi_{N_i^P, F_j} = 1,$
$$\tag{18b}$$

$R_{N_i^T, F_j} \geq R_{th}^{N_i}, \ R_{F_j, N_i^T} \geq R_{th}^{F_j}, \ \text{if } \Psi_{N_i^T, F_j} = 1, \tag{18c}$

$E_{N_i^P} \geq E_{th}^{N_i}, \ \text{if } \Psi_{N_i^P, F_j} = 1, \tag{18d}$

$E_{N_i^T} \geq E_{th}^{N_i}, \ \text{if } \Psi_{N_i^T, F_j} = 1, \tag{18e}$

$\tau_{N_i^T, F_j} + 2\widetilde{\tau}_{N_i^T, F_j} \leq t, \ \text{if } \Psi_{N_i^T, F_j} = 1, \tag{18f}$

$$\sum_{N_i^P \in \mathcal{N}^P} \Psi_{N_i^P, F_j} + \sum_{N_i^T \in \mathcal{N}^T} \Psi_{N_i^T, F_j} = 1, \ \forall F_j, \tag{18g}$$

$$\sum_{F_j \in \mathcal{F}} \Psi_{N_i^P, F_j} + \sum_{F_j \in \mathcal{F}} \Psi_{N_i^T, F_j} = 1, \ \forall N_i^P, \ \forall N_i^T, \tag{18h}$$

$\Psi_{N_i^P, F_j}, \Psi_{N_i^T, F_j} \in \{0, 1\}, \ \forall N_i^P, \ \forall N_i^T, \ \forall F_j, \tag{18i}$

$0 \leq \alpha_{N_i^P, F_j} \leq 1, 0 \leq \alpha_{N_i^T, F_j} \leq 1, \ \forall N_i^P, \ \forall N_i^T, \forall F_j, \tag{18j}$

$0 \leq \rho_{N_i^P, F_j} \leq 1, \ 0 \leq \tau_{N_i^T, F_j}, \widetilde{\tau}_{N_i^T, F_j}$
$$\leq t, \forall N_i^P, \ \forall N_i^T, \ \forall F_j, \tag{18k}$$

where $\Psi = [\Psi_1, \Psi_2]_{I \times I}$ is the user pairing matrix, $\alpha_1 = [\alpha_{N_i^P, F_j}]_{I_1 \times I}$ and $\alpha_2 = [\alpha_{N_i^T, F_j}]_{I_2 \times I}$ denote the power allocation matrices, $\rho = [\rho_{N_i^P, F_j}]_{I_1 \times I}$ is the PS control matrix, $\tau = [\tau_{N_i^T, F_j}]_{I_2 \times I}$ and $\widetilde{\tau} = [\widetilde{\tau}_{N_i^T, F_j}]_{I_2 \times I}$ represent the TS control matrices. Constraints (18b) and (18c) are imposed to guarantee the achievable rates of the NUs and the FUs are larger than their minimum data rate requirements. Note that $R_{th}^{N_i}$ and $R_{th}^{F_j}$ respectively denote the minimum data rates required by the NUs and the FUs. Constraints (18d) and (18e) represent the minimum required harvested energy $E_{th}^{N_i}$ of the NUs. Constraint (18f) ensures that the transmission time of a matched TSU-FU pair cannot exceed the available time t. Constraints (18g) and (18h) ensure each FU can be assisted by one NU, and each NU can be paired with one FU. Constraints (18i), (18j) and (18k) are respectively the feasible regions of the user pairing indicators, the power allocation coefficients, and the PS and TS factors.

The formulated problem $\mathcal{OP}$ involves the continuous resource allocation variables $\{\alpha_1, \alpha_2, \rho, \tau, \widetilde{\tau}\}$ and the binary user pairing variable Ψ. Besides, there exist the strong coupling of the optimization variables and the intra-pair interference of a NOMA pair. As a consequence, $\mathcal{OP}$ is a non-convex MINLP problem that is challenging to solve. Next, we will develop an efficient algorithm to solve this problem.

III. JOINT DESIGN OF USER PAIRING AND RESOURCE ALLOCATION

In this section, we design a joint user pairing and resource allocation algorithm for the general cooperative SWIPT NOMA system with coexisting PSUs and TSUs. Since the existence of continuous and binary variables in $\mathcal{OP}$ is rather difficult to tackle, we leverage the concept of the bi-level optimization and decompose $\mathcal{OP}$ into an inner resource allocation problem and an outer user pairing problem. The inner problem corresponds

to a sum-rate maximization problem concerning the resource allocation variables under given user pairing relationships. The outer problem corresponds to maximizing the sum of achievable rates with respect to (w.r.t.) the user pairing variable. Consequently, the proposed algorithm has two steps, which is shown as follows:

- The first step aims to find out a resource allocation policy under a fixed user pairing variable.
- The second step is to achieve the optimal user pairing relationships between the NUs and the FUs with the resource allocation policy obtained by the first step.

A. Inner Resource Allocation Problem

For the inner resource allocation problem, there is no binary variable. However, the strong coupling of the resource allocation variables and the presence of intra-pair interference in (10) and (17) make this problem still intricate to solve. To overcome this difficulty, we apply the BCD method and partition the resource allocation variables into two blocks: the power allocation block and the PS and TS control block. Correspondingly, the subproblem of power allocation and that of PS and TS control need to be solved. Besides, we note that the two subproblems are optimized iteratively until a satisfactory convergence is achieved. Subsequently, we will present the details of solving the two resource allocation subproblems.

1) Power Allocation Subproblem: For fixed PS and TS factors, we first optimize the power allocation variables $\{\alpha_{N_i^P, F_j}, \alpha_{N_i^T, F_j}\}$. As a consequence, the power allocation subproblem can be expressed as

$$\mathcal{OP}_1 : \max_{\alpha_{N_i^P, F_j}, \alpha_{N_i^T, F_j}} \sum_{\{N_i^P, F_j\} \in \Omega^P} (R_{N_i^P, F_j} + R_{F_j, N_i^P})$$

$$+ \sum_{\{N_i^T, F_j\} \in \Omega^T} (R_{N_i^T, F_j} + R_{F_j, N_i^T}) \quad (19a)$$

$$\text{s.t.} \quad (18b), \ (18c), \ (18j). \quad (19b)$$

where $\Omega^P = \{\forall N_i^P \in \mathcal{N}^P, \forall F_j \in \mathcal{F} \mid \Psi_{N_i^P, F_j} = 1\}$ and $\Omega^T = \{\forall N_i^T \in \mathcal{N}^T, \forall F_j \in \mathcal{F} \mid \Psi_{N_i^T, F_j} = 1\}$ denote matched PSU-FU pairs and matched TSU-FU pairs, respectively. It can be observed that $R_{N_i^P, F_j}$ and $R_{N_i^T, F_j}$ are respectively concave w.r.t. $\alpha_{N_i^P, F_j}$ and $\alpha_{N_i^T, F_j}$, while it is intractable to deal with R_{F_j, N_i^P} and R_{F_j, N_i^T} due to the existence of a minimum operation. In this respect, auxiliary variables $\gamma_{F_j, N_i^P} = \min\{\gamma_{N_i^P, x_{F_j}}^{(1)}, \gamma_{F_j, x_{F_j}}^{(1)} + \gamma_{F_j, x_{F_j}}^{(2)}\}$ and $\gamma_{F_j, N_i^T} = \min\{\gamma_{N_i^T, x_{F_j}}^{(1)}, \gamma_{F_j, x_{F_j}}^{(1)'} + \gamma_{F_j, x_{F_j}}^{(2)'}\}$ are introduced. Accordingly, $\gamma_{F_j, N_i^P} \leq \gamma_{N_i^P, x_{F_j}}^{(1)}$ and $\gamma_{F_j, N_i^P} \leq \gamma_{F_j, x_{F_j}}^{(1)} + \gamma_{F_j, x_{F_j}}^{(2)}$ are satisfied for γ_{F_j, N_i^P}, which leads to

$$\alpha_{N_i^P, F_j} \gamma_{F_j, N_i^P} \rho_{N_i^P, F_j} |h_{S, N_i^P}|^2 + \frac{\sigma^2}{P_S} \gamma_{F_j, N_i^P} \\ - \rho_{N_i^P, F_j} (1 - \alpha_{N_i^P, F_j}) |h_{S, N_i^P}|^2 \leq 0, \quad (20)$$

$$\alpha_{N_i^P, F_j} \gamma_{F_j, N_i^P} |h_{S, F_j}|^2 - \alpha_{N_i^P, F_j} |h_{S, F_j}|^2 \gamma_{F_j, x_{F_j}}^{(2)} \\ + \frac{\sigma^2}{P_S} (\gamma_{F_j, N_i^P} - \gamma_{F_j, x_{F_j}}^{(2)}) - (1 - \alpha_{N_i^P, F_j}) |h_{S, F_j}|^2 \leq 0. \quad (21)$$

Similarly, $\gamma_{F_j, N_i^T} \leq \gamma_{N_i^T, x_{F_j}}^{(1)}$ and $\gamma_{F_j, N_i^T} \leq \gamma_{F_j, x_{F_j}}^{(1)'} + \gamma_{F_j, x_{F_j}}^{(2)'}$ also should be maintained for γ_{F_j, N_i^T}. On this basis, we have the following inequations:

$$\alpha_{N_i^T, F_j} \gamma_{F_j, N_i^T} |h_{S, N_i^T}|^2 + \frac{\sigma^2}{P_S} \gamma_{F_j, N_i^T} \\ - (1 - \alpha_{N_i^T, F_j}) |h_{S, N_i^T}|^2 \leq 0, \quad (22)$$

$$\alpha_{N_i^T, F_j} \gamma_{F_j, N_i^T} |h_{S, F_j}|^2 - \alpha_{N_i^T, F_j} |h_{S, F_j}|^2 \gamma_{F_j, x_{F_j}}^{(2)'} \\ + \frac{\sigma^2}{P_S} (\gamma_{F_j, N_i^T} - \gamma_{F_j, x_{F_j}}^{(2)'}) - (1 - \alpha_{N_i^T, F_j}) |h_{S, F_j}|^2 \leq 0. \quad (23)$$

Note that $\gamma_{F_j, x_{F_j}}^{(2)}$ and $\gamma_{F_j, x_{F_j}}^{(2)'}$ are constants since they are irrelevant to the power allocation variables. Nevertheless, the introduced variable γ_{F_j, N_i^P} and the power allocation variable $\alpha_{N_i^P, F_j}$ are coupled together as a bilinear function in (20) and (21). In (22) and (23), γ_{F_j, N_i^T} and $\alpha_{N_i^T, F_j}$ are also coupled together. The Hessian matrices of bilinear functions are neither positive nor negative semi-definite matrices. Hence, bilinear functions are neither convex nor concave in general. To handle the bilinear terms on the left-hand sides of (20)–(23), we employ the following transformations

$$\alpha_{N_i^P, F_j} \gamma_{F_j, N_i^P} \\ = \frac{1}{4} \left[\left(\alpha_{N_i^P, F_j} + \gamma_{F_j, N_i^P} \right)^2 - \left(\alpha_{N_i^P, F_j} - \gamma_{F_j, N_i^P} \right)^2 \right], \quad (24)$$

$$\alpha_{N_i^T, F_j} \gamma_{F_j, N_i^T} \\ = \frac{1}{4} \left[\left(\alpha_{N_i^T, F_j} + \gamma_{F_j, N_i^T} \right)^2 - \left(\alpha_{N_i^T, F_j} - \gamma_{F_j, N_i^T} \right)^2 \right]. \quad (25)$$

With the above transformations, the successive convex approximation (SCA) method [31] is then applied to replace $\alpha_{N_i^P, F_j} \gamma_{F_j, N_i^P}$ and $\alpha_{N_i^T, F_j} \gamma_{F_j, N_i^T}$ by their convex upper approximation functions. To be specific, based on the first-order Taylor series expansion, the lower bounds of $(\alpha_{N_i^P, F_j} - \gamma_{F_j, N_i^P})^2$ and $(\alpha_{N_i^T, F_j} - \gamma_{F_j, N_i^T})^2$ can be respectively obtained around any feasible points $(\alpha_{N_i^P, F_j}^{(n)}, \gamma_{F_j, N_i^P}^{(n)})$ and $(\alpha_{N_i^T, F_j}^{(n)}, \gamma_{F_j, N_i^T}^{(n)})$ satisfying the constraints of problem $\mathcal{OP}_1$ as

$$(\alpha_{N_i^P, F_j} - \gamma_{F_j, N_i^P})^2 \geq f(\alpha_{N_i^P, F_j}, \gamma_{F_j, N_i^P}, \alpha_{N_i^P, F_j}^{(n)}, \gamma_{F_j, N_i^P}^{(n)}) \\ \triangleq (\alpha_{N_i^P, F_j}^{(n)} - \gamma_{F_j, N_i^P}^{(n)})^2 + 2(\alpha_{N_i^P, F_j}^{(n)} - \gamma_{F_j, N_i^P}^{(n)}) \\ \times [(\alpha_{N_i^P, F_j} - \alpha_{N_i^P, F_j}^{(n)}) - (\gamma_{F_j, N_i^P} - \gamma_{F_j, N_i^P}^{(n)})], \quad (26)$$

$$(\alpha_{N_i^T,F_j} - \gamma_{F_j,N_i^T})^2 \geq g(\alpha_{N_i^T,F_j}, \gamma_{F_j,N_i^T}, \alpha_{N_i^T,F_j}^{(n)}, \gamma_{F_j,N_i^T}^{(n)})$$
$$\triangleq (\alpha_{N_i^T,F_j}^{(n)} - \gamma_{F_j,N_i^T}^{(n)})^2 + 2(\alpha_{N_i^T,F_j}^{(n)} - \gamma_{F_j,N_i^T}^{(n)})$$
$$\times [(\alpha_{N_i^T,F_j} - \alpha_{N_i^T,F_j}^{(n)}) - (\gamma_{F_j,N_i^T} - \gamma_{F_j,N_i^T}^{(n)})]. \tag{27}$$

Based on (26) and (27), the left-hand sides of (20)–(23) can be approximated by their convex upper bounds. Therefore, (20)–(23) can be transformed into tractable forms which are presented in (28) at the bottom of this page. Accordingly, $\mathcal{OP}_1$ can be approximately reformulated as

$$\mathcal{OP}_1': \max_{\substack{\alpha_{N_i^P,F_j},\gamma_{F_j,N_i^P}, \\ \alpha_{N_i^T,F_j},\gamma_{F_j,N_i^T}}} \sum_{\{N_i^P,F_j\}\in\Omega^P} \left(R_{N_i^P,F_j} + \frac{t}{2}\log_2(1+\gamma_{F_j,N_i^P}) \right)$$
$$+ \sum_{\{N_i^T,F_j\}\in\Omega^T} (R_{N_i^T,F_j} + \tilde{\tau}_{N_i^T,F_j}\log_2(1+\gamma_{F_j,N_i^T})) \tag{29a}$$

s.t. $R_{N_i^P,F_j} \geq R_{th}^{N_i}, \quad \frac{t}{2}\log_2(1+\gamma_{F_j,N_i^P})$

$$>= R_{th}^{F_j}, \text{ if } \Psi_{N_i^P,F_j}=1, \tag{29b}$$

$$R_{N_i^T,F_j} \geq R_{th}^{N_i}, \text{ if } \Psi_{N_i^T,F_j}=1, \tag{29c}$$

$$\tilde{\tau}_{N_i^T,F_j}\log_2(1+\gamma_{F_j,N_i^T})) \geq R_{th}^{F_j}, \text{ if } \Psi_{N_i^T,F_j}=1, \tag{29d}$$

$$(18j), \ (28), \ \gamma_{F_j,N_i^P} \geq 0, \ \gamma_{F_j,N_i^T} \geq 0. \tag{29e}$$

Obviously, the objective function in (29a) is a concave function while the constraints in (29b)–(29e) restrict the convex sets of the optimization variables in $\mathcal{OP}_1'$. Therefore, $\mathcal{OP}_1'$ is a convex optimization problem, which can be efficiently solved by standard convex optimization solvers, such as CVX [32]. Moreover, to tighten the upper bounds of the left-hand sides of (28), as shown at the bottom of this page, we develop an iterative algorithm which is presented in Algorithm 1. The essence of Algorithm 1 is updating $(\alpha_{N_i^P,F_j}^{(n)}, \gamma_{F_j,N_i^P}^{(n)})$ and $(\alpha_{N_i^T,F_j}^{(n)}, \gamma_{F_j,N_i^T}^{(n)})$ to achieve tightened upper bounds iteratively. In particular, the

---

Algorithm 1: SCA-Based Algorithm to Solve $\mathcal{OP}_1$.

1: **Initialization:** Set the maximum number of iterations n_{max} and the iteration index $n=0$. Initialize the feasible parameters $(\alpha_{N_i^P,F_j}^{(n)}, \gamma_{F_j,N_i^P}^{(n)})$ and $(\alpha_{N_i^T,F_j}^{(n)}, \gamma_{F_j,N_i^T}^{(n)})$ that satisfy the constraints of problem $\mathcal{OP}_1$.
2: **repeat**
3:     $n=n+1$.
4:     Solve $\mathcal{OP}_1'$ using standard convex optimization tools and compute the optimal solution of $\mathcal{OP}_1'$.
5:     Denote the optimal solution of $\mathcal{OP}_1'$ as $\alpha_{N_i^P,F_j}'$, γ_{F_j,N_i^P}', $\alpha_{N_i^T,F_j}'$, and γ_{F_j,N_i^T}'.
6:     Update the feasible parameters as $\alpha_{N_i^P,F_j}^{(n)} \leftarrow \alpha_{N_i^P,F_j}'$, $\gamma_{F_j,N_i^P}^{(n)} \leftarrow \gamma_{F_j,N_i^P}'$, $\alpha_{N_i^T,F_j}^{(n)} \leftarrow \alpha_{N_i^T,F_j}'$, and $\gamma_{F_j,N_i^T}^{(n)} \leftarrow \gamma_{F_j,N_i^T}'$.
7: **until** Convergence or $n >= n_{max}$.
8: **Output:** $\alpha_{N_i^P,F_j}'$, γ_{F_j,N_i^P}', $\alpha_{N_i^T,F_j}'$, and γ_{F_j,N_i^T}'.

---

values of $\alpha_{N_i^P,F_j}^{(n)}$, $\gamma_{F_j,N_i^P}^{(n)}$, $\alpha_{N_i^T,F_j}^{(n)}$, and $\gamma_{F_j,N_i^T}^{(n)}$ can be respectively updated by the optimum solutions of $\alpha_{N_i^P,F_j}$, γ_{F_j,N_i^P}, $\alpha_{N_i^T,F_j}$, and γ_{F_j,N_i^T} at the n-th iteration. This process is repeated iteratively until convergence. Additionally, we provide Theorem 1 to illustrate the convergence of Algorithm 1.

Theorem 1: Algorithm 1 converges to the Karush-Kuhn-Tucker (KKT) point of the original problem $\mathcal{OP}_1$.

Proof: Please see Appendix A. ∎

2) PS and TS Control Subproblem: Then, we investigate the optimization of PS and TS control under fixed power allocation coefficients $\{\alpha_{N_i^P,F_j}, \alpha_{N_i^T,F_j}\}$. Accordingly, we need to solve the following subproblem:

$$\mathcal{OP}_2: \max_{\substack{\rho_{N_i^P,F_j}, \\ \tau_{N_i^T,F_j},\tilde{\tau}_{N_i^T,F_j}}} \sum_{\{N_i^P,F_j\}\in\Omega^P} (R_{N_i^P,F_j} + R_{F_j,N_i^P})$$
$$+ \sum_{\{N_i^T,F_j\}\in\Omega^T} (R_{N_i^T,F_j} + R_{F_j,N_i^T}) \tag{30a}$$

$$\frac{1}{4}\left[\left(\alpha_{N_i^P,F_j} + \gamma_{F_j,N_i^P}\right)^2 - f\left(\alpha_{N_i^P,F_j}, \gamma_{F_j,N_i^P}, \alpha_{N_i^P,F_j}^{(n)}, \gamma_{F_j,N_i^P}^{(n)}\right)\right]\rho_{N_i^P,F_j}|h_{S,N_i^P}|^2 + \frac{\sigma^2}{P_S}\gamma_{F_j,N_i^P}$$
$$-\rho_{N_i^P,F_j}(1-\alpha_{N_i^P,F_j})|h_{S,N_i^P}|^2 \leq 0,$$
$$\frac{1}{4}\left[\left(\alpha_{N_i^P,F_j} + \gamma_{F_j,N_i^P}\right)^2 - f\left(\alpha_{N_i^P,F_j}, \gamma_{F_j,N_i^P}, \alpha_{N_i^P,F_j}^{(n)}, \gamma_{F_j,N_i^P}^{(n)}\right)\right]|h_{S,F_j}|^2 - \alpha_{N_i^P,F_j}|h_{S,F_j}|^2\gamma_{F_j,x_{F_j}}^{(2)}$$
$$+\frac{\sigma^2}{P_S}(\gamma_{F_j,N_i^P} - \gamma_{F_j,x_{F_j}}^{(2)}) - (1-\alpha_{N_i^P,F_j})|h_{S,F_j}|^2 \leq 0.$$
$$\frac{1}{4}\left[\left(\alpha_{N_i^T,F_j} + \gamma_{F_j,N_i^T}\right)^2 - g\left(\alpha_{N_i^T,F_j}, \gamma_{F_j,N_i^T}, \alpha_{N_i^T,F_j}^{(n)}, \gamma_{F_j,N_i^T}^{(n)}\right)\right]|h_{S,N_i^T}|^2 + \frac{\sigma^2}{P_S}\gamma_{F_j,N_i^T}$$
$$-(1-\alpha_{N_i^T,F_j})|h_{S,N_i^T}|^2 \leq 0,$$
$$\frac{1}{4}\left[\left(\alpha_{N_i^T,F_j} + \gamma_{F_j,N_i^T}\right)^2 - g\left(\alpha_{N_i^T,F_j}, \gamma_{F_j,N_i^T}, \alpha_{N_i^T,F_j}^{(n)}, \gamma_{F_j,N_i^T}^{(n)}\right)\right]|h_{S,F_j}|^2 - \alpha_{N_i^T,F_j}|h_{S,F_j}|^2\gamma_{F_j,x_{F_j}}^{(2)'} + \frac{\sigma^2}{P_S}(\gamma_{F_j,N_i^T} - \gamma_{F_j,x_{F_j}}^{(2)'})$$
$$-(1-\alpha_{N_i^T,F_j})|h_{S,F_j}|^2 \leq 0. \tag{28}$$

s.t. (18b)–(18f), (18k). (30b)

In $\mathcal{OP}_2$, $R_{N_i^P, F_j}$ is a concave function of $\rho_{N_i^P, F_j}$ and $R_{N_i^T, F_j}$ is a linear function of $\tilde{\tau}_{N_i^T, F_j}$. Thus, the constraints related to $\rho_{N_i^P, F_j}$ and $R_{N_i^T, F_j}$ are tractable. And the main challenge of solving $\mathcal{OP}_2$ lies in tackling the minimum operations in R_{F_j, N_i^P} and R_{F_j, N_i^T}. To overcome this difficulty, we employ different methods to deal with the minimum operations. Specifically, we initially deal with R_{F_j, N_i^P} by introducing a new auxiliary variable $\overline{\gamma}_{F_j, N_i^P} = \min\{\gamma_{N_i^P, x_{F_j}}^{(1)}, \gamma_{F_j, x_{F_j}}^{(1)} + \gamma_{F_j, x_{F_j}}^{(2)}\}$. On this basis, we have

$$\rho_{N_i^P, F_j} \overline{\gamma}_{F_j, N_i^P} \alpha_{N_i^P, F_j} |h_{S, N_i^P}|^2 + \frac{\sigma^2}{P_S} \overline{\gamma}_{F_j, N_i^P} \\ - \rho_{N_i^P, F_j}(1 - \alpha_{N_i^P, F_j}) |h_{S, N_i^P}|^2 \le 0, \quad (31)$$

$$\gamma_{F_j, x_{F_j}}^{(1)} + \frac{\eta(1 - \rho_{N_i^P, F_j})|h_{S, N_i^P}|^2 |h_{N_i^P, F_j}|^2}{\frac{\sigma^2}{P_S}} \ge \overline{\gamma}_{F_j, N_i^P}. \quad (32)$$

Note that $\gamma_{F_j, x_{F_j}}^{(1)}$ is independent on $\rho_{N_i^P, F_j}$, and thus (32) is a linear constraint. To overcome the coupling relationship between $\rho_{N_i^P, F_j}$ and $\overline{\gamma}_{F_j, N_i^P}$ in (31), we exploit the upper bound of $\rho_{N_i^P, F_j} \overline{\gamma}_{F_j, N_i^P}$ and approximate (31) as

$$h(\rho_{N_i^P, F_j}, \overline{\gamma}_{F_j, N_i^P}, \widehat{\rho}_{N_i^P, F_j}, \widehat{\gamma}_{F_j, N_i^P}) \alpha_{N_i^P, F_j} |h_{S, N_i^P}|^2 \\ + \frac{\sigma^2}{P_S} \overline{\gamma}_{F_j, N_i^P} - \rho_{N_i^P, F_j}(1 - \alpha_{N_i^P, F_j}) |h_{S, N_i^P}|^2 \le 0, \quad (33)$$

where

$$h(\rho_{N_i^P, F_j}, \overline{\gamma}_{F_j, N_i^P}, \widehat{\rho}_{N_i^P, F_j}, \widehat{\gamma}_{F_j, N_i^P}) = \frac{1}{4}(\rho_{N_i^P, F_j} + \overline{\gamma}_{F_j, N_i^T})^2 \\ - \frac{1}{4}(\widehat{\rho}_{N_i^P, F_j} - \widehat{\gamma}_{F_j, N_i^P})^2 - \frac{1}{2}(\widehat{\rho}_{N_i^P, F_j} - \widehat{\gamma}_{F_j, N_i^P}) \\ \times [(\rho_{N_i^P, F_j} - \widehat{\rho}_{N_i^P, F_j}) - (\overline{\gamma}_{F_j, N_i^P} - \widehat{\gamma}_{F_j, N_i^P})]. \quad (34)$$

Here, $\widehat{\rho}_{N_i^P, F_j}$ and $\widehat{\gamma}_{F_j, N_i^P}$ are feasible parameters which satisfy the constraints of $\mathcal{OP}_2$.

Subsequently, we separately analyze two cases to deal with the non-concave property of R_{F_j, N_i^T}, i.e., $\gamma_{N_i^T, x_{F_j}}^{(1)} \le \gamma_{F_j, x_{F_j}}^{(1)'} + \gamma_{F_j, x_{F_j}}^{(2)'}$ and $\gamma_{N_i^T, x_{F_j}}^{(1)} \ge \gamma_{F_j, x_{F_j}}^{(1)'} + \gamma_{F_j, x_{F_j}}^{(2)'}$. For the two cases, $\mathcal{OP}_2$ can be respectively rewritten as $\mathcal{OP}_2'$ and $\mathcal{OP}_2''$, which are presented in (35) and (36) as shown at the bottom this page. In $\mathcal{OP}_2'$, the objective function is a concave function and the constraints restrict the convex sets of the optimization variables. Hence, $\mathcal{OP}_2'$ can be easily proved to be a convex optimization problem. Besides, we provide Theorem 2 to demonstrate $\mathcal{OP}_2''$ is also a convex optimization problem. As a result, both $\mathcal{OP}_2'$ and $\mathcal{OP}_2''$ can be solved by CVX. To tighten the approximation of (33), parameters $\widehat{\rho}_{N_i^P, F_j}$ and $\widehat{\gamma}_{F_j, N_i^P}$ are iteratively updated by the corresponding optimal solutions. To proceed this operation, we can directly employ Algorithm 1 by simply replacing problem $\mathcal{OP}_1'$ by problem $\mathcal{OP}_2'$ and $\mathcal{OP}_2''$ as well as changing relevant initializations and updates. Since $\mathcal{OP}_2$ comprises the two cases, the optimal value of the objective function in $\mathcal{OP}_2$ can be given by $\max\{R_2', R_2''\}$, where R_2' is the optimal value of the objective function in $\mathcal{OP}_2'$ and R_2'' represents the optimal objective value in $\mathcal{OP}_2''$.

Theorem 2: $\mathcal{OP}_2''$ is a convex optimization problem.

Proof: Please see Appendix B. ∎

3) BCD-Based Resource Allocation Algorithm: Now, the solutions to the two resource allocation subproblems are obtained. Then, we propose a BCD-based iterative algorithm to jointly optimize the two subproblems. Note that the initialization of Algorithm 2 must satisfy all the constraints of $\mathcal{OP}$. Besides, at each iteration l of the proposed Algorithm 2, the power allocation variables and the PS and TS control variables are updated in turn with the rest variables as constants. Namely, given PS and TS control variables, the power allocation variables are calculated by solving $\mathcal{OP}_1'$. Subsequently, with the obtained power allocation variables, the PS and TS control variables are calculated by solving $\mathcal{OP}_2'$ and $\mathcal{OP}_2''$. This iterative process terminates until convergence and the output is a resource allocation policy $\{\alpha_{N_i^P, F_j}^*, \alpha_{N_i^T, F_j}^*, \rho_{N_i^P, F_j}^*, \tau_{N_i^T, F_j}^*, \tilde{\tau}_{N_i^T, F_j}^*\}$ for given user pairing relationships between the NUs and the FUs.

$$\mathcal{OP}_2': \max_{\substack{\rho_{N_i^P, F_j}, \overline{\gamma}_{F_j, N_i^P} \\ \tau_{N_i^T, F_j}, \tilde{\tau}_{N_i^T, F_j}}} \sum_{\{N_i^P, F_j\} \in \Omega^P} \left(R_{N_i^P, F_j} + \frac{t}{2}\log_2(1 + \overline{\gamma}_{F_j, N_i^P})\right) + \sum_{\{N_i^T, F_j\} \in \Omega^T} \left(R_{N_i^T, F_j} + \tilde{\tau}_{N_i^T, F_j}\log_2(1 + \gamma_{N_i^T, x_{F_j}}^{(1)})\right)$$

s.t. $R_{N_i^P, F_j} \ge R_{th}^{N_i}$, $\frac{t}{2}\log_2(1 + \gamma_{F_j, N_i^P}) \ge R_{th}^{F_j}$, if $\Psi_{N_i^P, F_j} = 1, R_{N_i^T, F_j} \ge R_{th}^{N_i}$, $\tilde{\tau}_{N_i^T, F_j}\log_2(1 + \gamma_{N_i^T, x_{F_j}}^{(1)}))$

$\ge R_{th}^{F_j}$, $\gamma_{N_i^T, x_{F_j}}^{(1)} \le \gamma_{F_j, x_{F_j}}^{(1)'} + \gamma_{F_j, x_{F_j}}^{(2)'}$, if $\Psi_{N_i^T, F_j} = 1, (18d)$–$(18f), (18k), (32), (33), \overline{\gamma}_{F_j, N_i^P} \ge 0.$ (35)

$$\mathcal{OP}_2'': \max_{\substack{\rho_{N_i^P, F_j}, \overline{\gamma}_{F_j, N_i^P} \\ \tau_{N_i^T, F_j}, \tilde{\tau}_{N_i^T, F_j}}} \sum_{\{N_i^P, F_j\} \in \Omega^P} \left(R_{N_i^P, F_j} + \frac{t}{2}\log_2(1 + \overline{\gamma}_{F_j, N_i^P})\right) + \sum_{\{N_i^T, F_j\} \in \Omega^T} \left(R_{N_i^T, F_j} + \tilde{\tau}_{N_i^T, F_j}\log_2(1 + \gamma_{F_j, x_{F_j}}^{(1)'} + \gamma_{F_j, x_{F_j}}^{(2)'})\right)$$

s.t. $R_{N_i^P, F_j} \ge R_{th}^{N_i}$, $\frac{t}{2}\log_2(1 + \gamma_{F_j, N_i^P}) \ge R_{th}^{F_j}$, if $\Psi_{N_i^P, F_j} = 1, R_{N_i^T, F_j} \ge R_{th}^{N_i}$, $\tilde{\tau}_{N_i^T, F_j}\log_2(1 + \gamma_{F_j, x_{F_j}}^{(1)'} + \gamma_{F_j, x_{F_j}}^{(2)'}))$

$\ge R_{th}^{F_j}$, $\gamma_{N_i^T, x_{F_j}}^{(1)'} > \gamma_{F_j, x_{F_j}}^{(1)'} + \gamma_{F_j, x_{F_j}}^{(2)'}$, if $\Psi_{N_i^T, F_j} = 1, (18d)$–$(18f), (18k), (32), (33), \overline{\gamma}_{F_j, N_i^P} \ge 0.$ (36)

Algorithm 2: BCD-Based Resource Allocation Algorithm to Solve the Inner Resource Allocation Problem.

1: **Initialization:** Set the maximum number of iterations l_{max} and the iteration index $l = 0$. Initialize $\alpha_{N_i^P,F_j}^{(0)}$, $\alpha_{N_i^T,F_j}^{(0)}$, $\rho_{N_i^P,F_j}^{(0)}$, $\tau_{N_i^T,F_j}^{(0)}$, and $\widetilde{\tau}_{N_i^T,F_j}^{(0)}$.

2: **repeat**

3:     $l = l + 1$.

4:     Given $\rho_{N_i^P,F_j}^{(l-1)}$, $\tau_{N_i^T,F_j}^{(l-1)}$ and $\widetilde{\tau}_{N_i^T,F_j}^{(l-1)}$, obtain the power allocation variables $\alpha_{N_i^P,F_j}^{(l)}$ and $\alpha_{N_i^T,F_j}^{(l)}$ by Algorithm 1.

5:     With the obtained $\alpha_{N_i^P,F_j}^{(l)}$ and $\alpha_{N_i^T,F_j}^{(l)}$ in the previous step, calculate the PS and TS control variables $\rho_{N_i^P,F_j}^{(l)}$, $\tau_{N_i^T,F_j}^{(l)}$, and $\widetilde{\tau}_{N_i^T,F_j}^{(l)}$ by solving $\mathcal{OP}_2'$ and $\mathcal{OP}_2''$.

6: **until** Convergence or $l \geq l_{max}$.

7:     Set $\alpha_{N_i^P,F_j}^* \leftarrow \alpha_{N_i^P,F_j}^{(l)}$, $\alpha_{N_i^T,F_j}^* \leftarrow \alpha_{N_i^T,F_j}^{(l)}$, $\rho_{N_i^P,F_j}^* \leftarrow \rho_{N_i^P,F_j}^{(l)}$, $\tau_{N_i^T,F_j}^* \leftarrow \tau_{N_i^T,F_j}^{(l)}$, and $\widetilde{\tau}_{N_i^T,F_j}^* \leftarrow \widetilde{\tau}_{N_i^T,F_j}^{(l)}$.

8: **Output:** $\alpha_{N_i^P,F_j}^*$, $\alpha_{N_i^T,F_j}^*$, $\rho_{N_i^P,F_j}^*$, $\tau_{N_i^T,F_j}^*$, and $\widetilde{\tau}_{N_i^T,F_j}^*$.

Besides, we provide the following theorem to demonstrate the convergence of Algorithm 2.

Theorem 3: Algorithm 2 is guaranteed to converge within limited iterations.

Proof: Please see Appendix C. ∎

B. Outer User Pairing Problem

Although the resource allocation policy is obtained, the outer user pairing is still a combinatory optimization problem. The optimal solution of pairing can be obtained using the exhaustive search method, but the computational complexity increases exponentially with the number of users [36]. As a result, this method is not practical, especially for large-scale IoT networks and WSNs. Hence, we propose a low-complexity user pairing strategy based on the characteristics of the outer problem of user pairing. Specifically, the outer user pairing problem can be given by

$$\mathcal{OP}_3: \max_{\mathbf{\Psi}} \sum_{F_j \in \mathcal{F}} \sum_{N_i^P \in \mathcal{N}^P} \Psi_{N_i^P,F_j} R_{N_i^P,F_j}^{\text{sum}*}$$

$$+ \sum_{F_j \in \mathcal{F}} \sum_{N_i^T \in \mathcal{N}^T} \Psi_{N_i^T,F_j} R_{N_i^T,F_j}^{\text{sum}*} \qquad (37a)$$

$$\text{s.t. } (18g), (18h), (18i). \qquad (37b)$$

where $R_{N_i^P,F_j}^{\text{sum}*} = R_{N_i^P,F_j}(\alpha_{N_i^P,F_j}^*, \rho_{N_i^P,F_j}^*) + R_{F_j,N_i^P}(\alpha_{N_i^P,F_j}^*, \rho_{N_i^P,F_j}^*)$ is the sum-rate of a matched PSU-FU pair and $R_{N_i^T,F_j}^{\text{sum}*} = R_{N_i^T,F_j}(\alpha_{N_i^T,F_j}^*, \tau_{N_i^T,F_j}^*, \widetilde{\tau}_{N_i^T,F_j}^*) + R_{F_j,N_i^T}(\alpha_{N_i^T,F_j}^*, \tau_{N_i^T,F_j}^*, \widetilde{\tau}_{N_i^T,F_j}^*)$ denotes the sum-rate of a matched
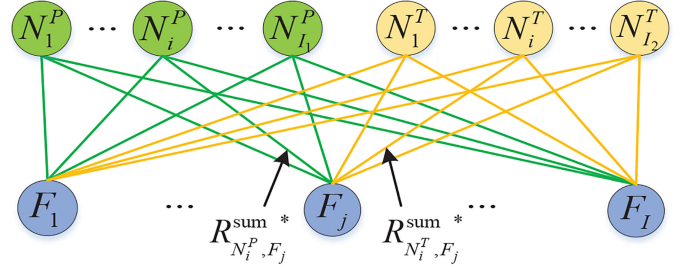

Fig. 2. A matched bipartite graph.

TSU-FU pair. Next, we aim to obtain optimal user pairing relationships between NUs and FUs with the obtained resource allocation strategy $\{\alpha_{N_i^P,F_j}^*, \alpha_{N_i^T,F_j}^*, \rho_{N_i^P,F_j}^*, \tau_{N_i^T,F_j}^*, \widetilde{\tau}_{N_i^T,F_j}^*\}$.

In this work, the user pairing problem can be regarded as a one-to-one matching problem between the set of the NUs and that of the FUs. Since we consider a general scenario consisting of two kinds of NUs, i.e., the PSUs and the TSUs, it is required to find the best matching relationships between the PSUs, the TSUs and the FUs to achieve the maximum objective value of $\mathcal{OP}_3$. To this end, we construct a bipartite graph $\Gamma = (\mathcal{N}^P, \mathcal{N}^T, \mathcal{F}, \mathcal{E}^P, \mathcal{E}^T)$ which is shown in Fig. 2. This bipartite graph contains the PSUs, the TSUs and the FUs, and these users can be seen as the vertices of the bipartite graph. Particularly, $\mathcal{N}^P = \{N_i^P | \forall N_i^P \in \mathcal{N}^P\}$, $\mathcal{N}^T = \{N_i^T | \forall N_i^T \in \mathcal{N}^T\}$ and $\mathcal{F} = \{F_j | \forall F_j \in \mathcal{F}\}$ represent the sets of the PSUs, the TSUs and the FUs, respectively. Besides, $\mathcal{E}^P = \{R_{N_i^P,F_j}^{\text{sum}*} | \forall N_i^P \in \mathcal{N}^P, \forall F_j \in \mathcal{F}\}$ denotes the weights of the edge between vertices N_i^P and F_j, and $\mathcal{E}^T = \{R_{N_i^T,F_j}^{\text{sum}*} | \forall N_i^T \in \mathcal{N}^T, \forall F_j \in \mathcal{F}\}$ represents the weights of the edge between vertices N_i^T and F_j. Based on the constructed bipartite graph, $\mathcal{OP}_3$ is cast into an MWBM problem, which can be efficiently solved by the Hungarian algorithm. To be specific, the Hungarian algorithm requires an $I \times I$ cost matrix $\mathbf{C}$ as an input and it is used to solve minimization problems. Accordingly, we define each element of the input cost matrix is $\frac{1}{R_{N_i^P,F_j}^{\text{sum}*}}$ or $\frac{1}{R_{N_i^T,F_j}^{\text{sum}*}}$. That is, when FU F_j is matched with PSU N_i^P, the corresponding input element $\mathbf{C}(i,j)$ is defined as $\frac{1}{R_{N_i^P,F_j}^{\text{sum}*}}$. Otherwise, the input element is $\frac{1}{R_{N_i^T,F_j}^{\text{sum}*}}$. Note that the elements of input cost matrix $\mathbf{C}$ are composed of both $\frac{1}{R_{N_i^P,F_j}^{\text{sum}*}}$ and $\frac{1}{R_{N_i^T,F_j}^{\text{sum}*}}$ due to the co-existence of PSUs and TSUs, which indicates the elements of $\mathbf{C}$ depend on the results of power allocation, PS and TS control in $\mathcal{OP}_1$ and $\mathcal{OP}_2$. Consequently, the elements of the cost matrix $\mathbf{C}$ are independent of the pairing relationships that already have been performed. On this basis, the Hungarian algorithm is provided with a square cost matrix as an input, and it can output an optimal user pairing matrix $\mathbf{\Psi}^*$ [37].

C. Convergence and Complexity Analysis

Till now, we have solved the problem $\mathcal{OP}$. To summarize, the overall procedure is presented in Algorithm 3. It can be seen that the essence of Algorithm 3 is using a two-step policy. Following this policy, the resource allocation solution can be obtained by

---

Algorithm 3: Proposed Two-Step User Pairing and Resource Allocation Algorithm.

1: **Input:** The configuration of the cooperative SWIPT NOMA system and the categories of the NUs.
2: **—First Step: Resource allocation**
3: Solve the power allocation subproblem $\mathcal{OP}_1$ by proposing the SCA-based algorithm in Algorithm 1.
4: Solve the PS and TS control subproblem $\mathcal{OP}_2$ by proposing the SCA-based algorithm.
5: Optimize power allocation as well as PS and TS control iteratively by proposing the BCD-based algorithm in Algorithm 2.
6: **—Second Step: User pairing**
7: According to the resource allocation policy obtained from the first step, compute the cost matrix $\mathbf{C}$.
8: If FU F_j is matched with PSU N_i^P, the corresponding input element $\mathbf{C}(i, j)$ is $\frac{1}{R_{N_i^P, F_j}^{\text{sum}*}}$. If FU F_j is matched with TSU N_i^T, the input element is $\frac{1}{R_{N_i^T, F_j}^{\text{sum}*}}$.
9: Solve the optimal pairing matrix $\boldsymbol{\Psi}^*$ using the Hungarian algorithm with the cost matrix.
10: **Output:** A joint user pairing and resource allocation scheme.

---

using the SCA and BCD methods, and the user pairing problem is well tackled by the Hungarian algorithm. Subsequently, we analyze the convergence and computational complexity of the proposed algorithm.

Convergence Analysis: In Algorithm 3, the iterative process exists in solving inner resource allocation problem, i.e., the power allocation subproblem and the PS and TS control subproblem are iteratively optimized via an alternating optimization manner. The convergence of this process is proved in Theorem 3.

Complexity Analysis: The complexity of Algorithm 3 is theoretically analyzed as follows. The complexity of solving the outer user pairing by the Hungarian algorithm is $\mathcal{O}(I^3)$. Since the inner resource allocation problem is solved by the BCD method, the complexity of solving the inner resource allocation problem is a linear combination of the complexity of solving each subproblem. Specifically, $\mathcal{OP}_1$ and $\mathcal{OP}_2$ can be transformed into convex optimization problems that are solved by CVX. Therefore, the complexity of solving the inner resource allocation problem can be written as $\mathcal{O}(\ell(N_1 I^{3.5} \log^3(1/\epsilon) + N_2 I^{3.5} \log^3(1/\epsilon)))$, where N_1, N_2, and ℓ are respectively the iteration number of Algorithm 1, the SCA method, and the BCD method, and ϵ is the. As a result, the overall computation complexity of Algorithm 3 is $\mathcal{O}(\ell(N_1 I^{3.5} \log^3(1/\epsilon) + N_2 I^{3.5} \log^3(1/\epsilon)) + I^3)$. That is, Algorithm 3 can solve the formulated MINLP problem in polynomial time complexity.

IV. SIMULATION RESULTS

In the section, we present simulation results to evaluate the performance of the proposed JUPRA scheme in a general cooperative SWIPT NOMA system. The system parameter setup

follows the existing works [15] and [20]. Specifically, the channel power gains are modeled as $|h_{i,j}|^2 = \theta_{i,j} d_{i,j}^{-\beta}$ for $(i, j) \in \{(S, N_i^P), (S, N_i^T), (S, F_j), (N_i^P, F_j), (N_i^T, F_j)\}$, where $d_{i,j}$ is the distance between node i and node j, β represents the path-loss exponent, and $\theta_{i,j}$ refers to an exponentially distributed random variable with mean unity. The minimum data rates $R_{th}^{N_i}$ and $R_{th}^{F_j}$ are respectively set to be equal for the NUs and the FUs, i.e., $R_{th}^{N_i} = R_{th1}$ and $R_{th}^{F_j} = R_{th2}$. Unless other specified, we set the EH efficiency as $\eta = 0.5$, the path-loss exponent as $\beta = 3$, the number of users as 10, the minimum harvested energy requirement as -15 dBm, and $P_S/\sigma^2 = 25$ dB. To evaluate the performance of the proposed JUPRA scheme, we compare our scheme with the existing baseline schemes described as follows:

- Fixed power allocation scheme in [38]: In this scheme, cooperative NOMA pairs employ a fixed power allocation strategy, i.e., the amount of power allocated to each NU/FU is set fixed.
- Fixed PS and TS control scheme: PS factors and TS factors at the PSUs and the TSUs are set as fixed values, while user pairing and power allocation are jointly optimized to improve the network sum-rate.
- User pairing scheme in [15]: From the source, the nearest NU is paired with the farthest FU, the second nearest NU is paired with the second farthest FU, and so on.
- Non-cooperative NOMA scheme in [39]: The source simultaneously serves a matched NU and FU pair using NOMA. But the NUs don't perform as relays for assisting the communications between the source and the FUs, i.e., there is no cooperative transmission process.

A. Performance Comparison

In this subsection, we compare the proposed JUPRA scheme with the baseline schemes from different perspectives. Firstly, we present the network sum-rate achieved by all the schemes versus P_S/σ^2 in Fig. 3. It is evident that with the increase of P_S/σ^2, the sum-rates of users monotonously increases in all the schemes. This is because the increasing P_S/σ^2 makes more power available at the NUs and the FUs, which can enhance their achievable rates. Besides, it is observed that the proposed JUPRA scheme exhibits better performance than the baseline schemes in terms of the sum-rates of users, especially in the high P_S/σ^2 region. It can be attributed to the fact that in the proposed JUPRA scheme, the power is allocated dynamically to the NUs and the FUs, and the PS factors at the PSUs and the TS factors at the TSUs are controlled flexibly, which is opposed to the fixed power allocation scheme in [15] and the fixed PS and TS control scheme. Further, the user pairing is performed on basis of the channel gains of both source-user links and user-user links, while the user pairing scheme in [38] employs a static pairing strategy which only focuses on the channel gains of source-user links. Hence, the sum-rate of the proposed JUPRA scheme against P_S/σ^2 is higher than that of the user pairing scheme in [38]. Moreover, by comparing the proposed JUPRA scheme with the non-cooperative NOMA scheme in [39], it can be seen that adopting the cooperative transmission design between the
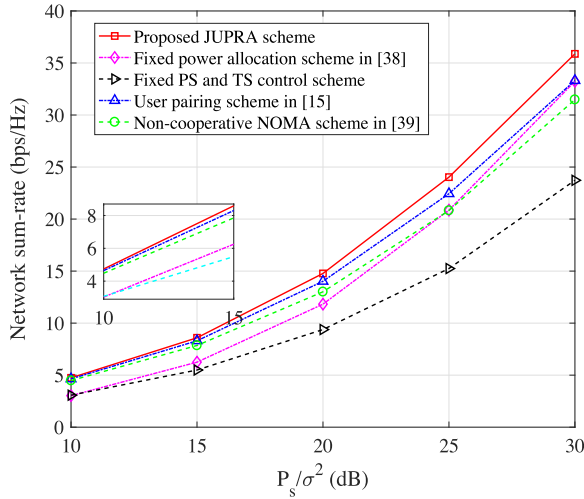
Fig. 3. Comparison of network sum-rate between JUPRA and baseline schemes under varying P_S/σ^2.
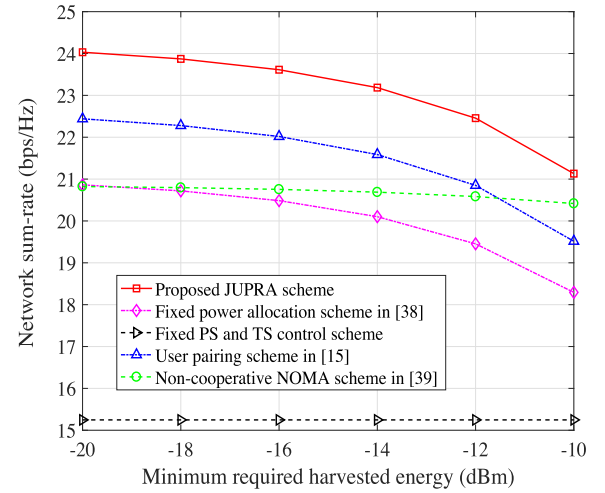

Fig. 5. Comparison of network sum-rate between JUPRA and baseline schemes under varying minimum required harvested energy of the NUs.
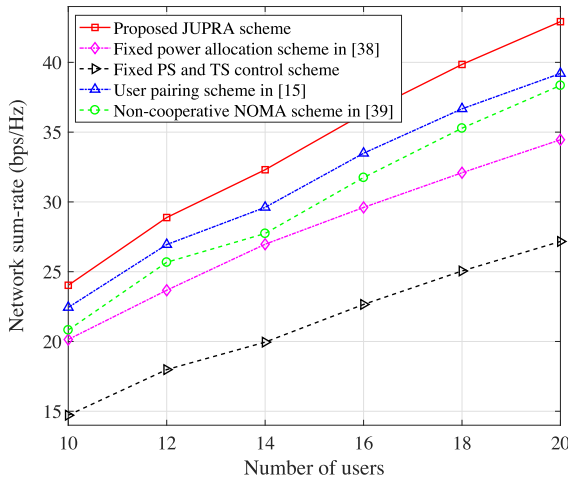

Fig. 4. Comparison of network sum-rate between JUPRA and baseline schemes under varying number of users.

NUs and the FUs is beneficial to improving the sum-rates of users.

Fig. 4 presents the simulation results of the network sum-rate against the number of users in different schemes. We can observe that the network sum-rates achieved by all the schemes increase with the number of users. This is because when the number of users increases, the NUs and the FUs have more opportunities to select their partners to form cooperative NOMA pairs, which is beneficial to improving the network sum-rate. Further, our proposed scheme achieves a higher network sum-rate than the baseline schemes. For instance, when the number of users is 20, the proposed JUPRA scheme respectively improves about 24.6%, 57.9%, 9.5%, and 11.9% in comparison to the fixed power allocation scheme in [15], the fixed PS and TS control scheme, the user pairing scheme in [38], and the non-cooperative NOMA scheme in [39]. The reason is the joint design of user pairing and resource allocation in our scheme comprehensively considers the factors that have impacts on sum-rate performance.

Fig. 5 depicts the comparison of the network sum-rate between the proposed JUPRA scheme and the baseline schemes under different minimum required harvested energy. Three observations can be remarked from Fig. 5. First, in all the schemes except for the fixed PS and TS control scheme, the network sum-rate monotonically decreases with the minimum harvested energy requirement. This observation is caused by a two-fold reason. On the one hand, for the PSUs, when the minimum harvested energy requirement increases, a larger portion of the received signal is allocated for performing EH. Consequently, the portion of the received signal for conducting ID declines, which decreases the achievable rates of the PSUs. On the other hand, for the TSUs, the time for performing EH has to increase to satisfy the minimum harvested energy requirement. Accordingly, the information transmission time declines and thus the achievable rates of the TSUs decrease. Second, the sum-rate in the fixed PS and TS control scheme keeps unchanged. The reason is the received signal split for performing EH at the PSUs and the EH time at the TSUs are not adaptive in this scheme. Third, the non-cooperative NOMA scheme in [39] has a slower downtrend than the proposed scheme, the fixed power allocation scheme in [15], and the user pairing scheme in [38]. This is due to the fact that no cooperation between the NUs and the FUs makes the achievable data rates of the FUs independent of the energy harvested by the NUs. Accordingly, when the minimum harvested energy requirement increases, the decreasing speed of the sum-rate achieved by the non-cooperative NOMA scheme in [39] is relatively flat.

Fig. 6 demonstrates the sum-rates of users under different path-loss exponent β. We can see that, for both the proposed JUPRA and the baseline schemes, the increasing β results in significant degradation of the network sum-rate. This is because, as the path-loss exponent increases, the achievable rates from S to the NUs, from S to the FUs, and from the NUs to the FUs decrease. Meanwhile, the energy harvested by the NUs also declines, which decreases the transmit powers for performing cooperative transmissions. As a result, the network sum-rate
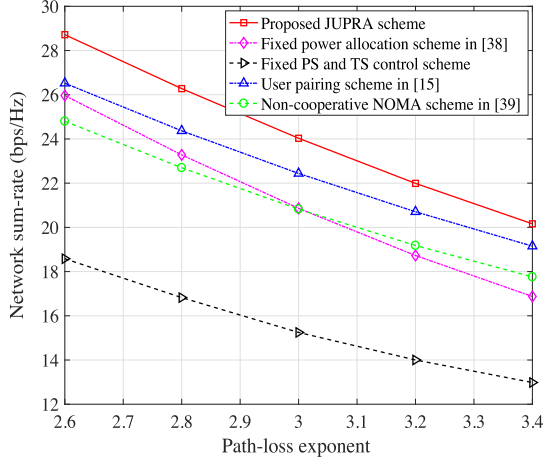
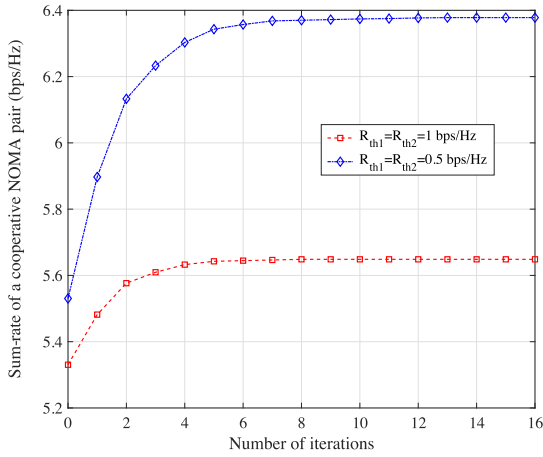Fig. 6. Comparison of network sum-rate between JUPRA and baseline schemes under varying path-loss exponent.

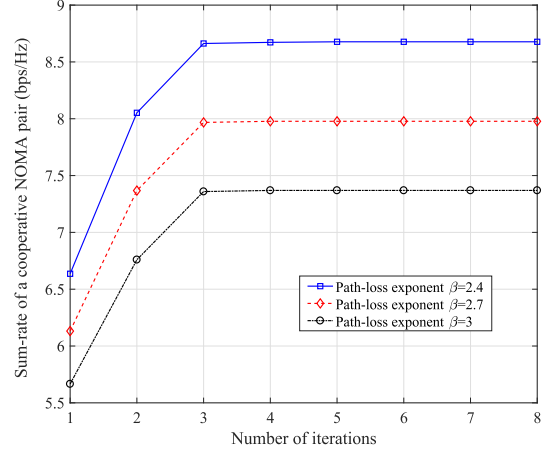Fig. 7. Convergence behavior of Algorithm 1 over different targeted rates of users.

Fig. 8. Convergence behavior of Algorithm 2 over different path-loss exponents.

observed that each sum-rate achieved by Algorithm 2 converges to a stable value with a fast convergence speed.

V. CONCLUSION

This paper studied the general cooperative SWIPT NOMA system, in which the NUs that have the capability of performing the PS or TS strategy can assist the information transmissions between the source and the FUs. In this system, a joint design of user pairing and resource allocation was mathematically formulated as a network sum-rate maximization problem subject to users' minimum requirements on data rate and harvested energy. To tackle the formulated MINLP problem, we proposed a two-step algorithm that decouples the formulated problem into an inner resource allocation problem and an outer user pairing problem. First, SCA and BCD-based algorithms were proposed to solve the inner resource allocation problem. On this basis, the Hungarian algorithm was then adopted to obtain an optimal pairing strategy between the NUs and the FUs. Besides, the convergence and computational complexity of the proposed algorithms were demonstrated. Finally, the simulation results showed that the proposed scheme outperforms some existing schemes in the literature. Investigating energy-efficient user pairing and resource allocation schemes under imperfect CSI and nonlinear EH models would be our future work.

APPENDIX A
THE PROOF OF THEOREM 1

According to [33], SCA ensures a non-decreasing sequence of objective values, because the solution obtained by solving $\mathcal{OP}_1$ at n-th iteration is a feasible point of problem $\mathcal{OP}_1$ at $(n + 1)$-th iteration. Besides, $\mathcal{OP}_1$ is upper bounded by a finite value due to the imposed constraints. Therefore, Algorithm 1 is guaranteed to converge.

Then, we prove the outcome of Algorithm 1 is the KKT point of $\mathcal{OP}_1$. For convenience, the left-hand sides of (20)–(23) are respectively denoted as $\mathcal{G}_1$, $\mathcal{G}_2$, $\mathcal{G}_3$, and $\mathcal{G}_4$. Besides, we denote the left-hand sides of (28) as $\widetilde{G}_1$, $\widetilde{G}_2$, $\widetilde{G}_3$, and $\widetilde{G}_4$, respectively. Following the results in [34], the proposed SCA-based algorithm

presents a decreasing trend. Besides, as the same observations in the above simulations, the comparison of the achievable sum-rates of users between our scheme and the baseline schemes illustrates the superiority of the proposed JUPRA scheme.

B. Convergence Analysis

Subsequently, we demonstrate the convergence of our proposed algorithms, and the iteration error tolerance is set as 10^{-5}. Firstly, we evaluate the convergence rate of Algorithm 1. A monotonic convergence state is observed from Fig. 7, which verifies Theorem 1. Besides, it can be observed that Algorithm 1 can converge to different values under different target data rates of users. Especially, the achievable data rate of $R_{th1}=0.5$bps/Hz is higher than that of $R_{th1}=1$bps/Hz. This is due to the fact that higher transmit power is allocated to the FUs to reach the target data rate $R_{th1}=1$bps/Hz, which indicates more power is wasted in combating poor channel conditions instead of contributing higher data rate if it is allocated to the NUs. In Fig. 8, we then evaluate the convergence behavior of Algorithm 2. The results are obtained under different path-loss exponents. It can be

can converge the KKT point of $\mathcal{OP}_1$ if the following conditions are all satisfied. For $k = 1$ and $k = 2$:

$$\widetilde{G}_k(\alpha_{N_i^P,F_j}, \gamma_{F_j,N_i^P}, \widetilde{\alpha}_{N_i^P,F_j}, \widetilde{\gamma}_{F_j,N_i^P}) \geq \mathcal{G}_k(\alpha_{N_i^P,F_j}, \gamma_{F_j,N_i^P}), \quad (38)$$

$$\widetilde{G}_k(\alpha_{N_i^P,F_j}, \gamma_{F_j,N_i^P}, \alpha_{N_i^P,F_j}^{(n)}, \gamma_{F_j,N_i^P}^{(n)})\Big|_{(\alpha_{N_i^P,F_j}^{(n)}, \gamma_{F_j,N_i^P}^{(n)})}$$
$$= \mathcal{G}_k(\alpha_{N_i^P,F_j}, \gamma_{F_j,N_i^P})\Big|_{(\alpha_{N_i^P,F_j}^{(n)}, \gamma_{F_j,N_i^P}^{(n)})}, \quad (39)$$

$$\frac{\partial \widetilde{G}_k(\alpha_{N_i^P,F_j}, \gamma_{F_j,N_i^P}, \alpha_{N_i^P,F_j}^{(n)}, \gamma_{F_j,N_i^P}^{(n)})}{\partial \alpha_{N_i^P,F_j}}\Big|_{(\alpha_{N_i^P,F_j}^{(n)}, \gamma_{F_j,N_i^P}^{(n)})}$$
$$= \frac{\nabla \mathcal{G}_k(\alpha_{N_i^P,F_j}, \gamma_{F_j,N_i^P})}{\partial \alpha_{N_i^P,F_j}}\Big|_{(\alpha_{N_i^P,F_j}^{(n)}, \gamma_{F_j,N_i^P}^{(n)})}, \quad (40)$$

$$\frac{\partial \widetilde{G}_k(\alpha_{N_i^P,F_j}, \gamma_{F_j,N_i^P}, \alpha_{N_i^P,F_j}^{(n)}, \gamma_{F_j,N_i^P}^{(n)})}{\partial \gamma_{N_i^P,F_j}}\Big|_{(\alpha_{N_i^P,F_j}^{(n)}, \gamma_{F_j,N_i^P}^{(n)})}$$
$$= \frac{\nabla \mathcal{G}_k(\alpha_{N_i^P,F_j}, \gamma_{F_j,N_i^P})}{\partial \gamma_{N_i^P,F_j}}\Big|_{(\alpha_{N_i^P,F_j}^{(n)}, \gamma_{F_j,N_i^P}^{(n)})}. \quad (41)$$

For $k = 3$ and $k = 4$, the required conditions are similar to the above (36)–(39). Besides, the expressions of $\nabla \widetilde{G}_3$ and $\nabla \mathcal{G}_3$ are respectively similar to that of $\nabla \widetilde{G}_1$ and $\nabla \mathcal{G}_1$, and the expressions of $\nabla \widetilde{G}_4$ and $\nabla \mathcal{G}_4$ are respectively similar to that of $\nabla \widetilde{G}_2$ and $\nabla \mathcal{G}_2$. Thus, the proof of the required conditions for $k = 3$ and $k = 4$ is omitted due to similarity.

Obviously, (36) is satisfied based on the process of deriving $\mathcal{OP}_1'$. According to (26), we can obtain $(\alpha_{N_i^P,F_j}^{(n)} - \gamma_{F_j,N_i^P}^{(n)})^2 = f(\alpha_{N_i^P,F_j}, \gamma_{F_j,N_i^P}, \alpha_{N_i^P,F_j}^{(n)}, \gamma_{F_j,N_i^P}^{(n)})|_{(\alpha_{N_i^P,F_j}^{(n)}, \gamma_{F_j,N_i^P}^{(n)})}$. Thus, we can conclude (37) is satisfied. Then, we drive the partial derivatives of $f(\alpha_{N_i^P,F_j}, \gamma_{F_j,N_i^P}, \alpha_{N_i^P,F_j}^{(n)}, \gamma_{F_j,N_i^P}^{(n)})$ and $(\alpha_{N_i^P,F_j} - \gamma_{F_j,N_i^P})^2$ as

$$\frac{\partial f(\alpha_{N_i^P,F_j}, \gamma_{F_j,N_i^P}, \alpha_{N_i^P,F_j}^{(n)}, \gamma_{F_j,N_i^P}^{(n)})}{\partial \alpha_{N_i^P,F_j}}\Big|_{(\alpha_{N_i^P,F_j}^{(n)}, \gamma_{F_j,N_i^P}^{(n)})}$$
$$= \frac{\partial(\alpha_{N_i^P,F_j} - \gamma_{F_j,N_i^P})^2}{\partial \alpha_{N_i^P,F_j}}\Big|_{(\alpha_{N_i^P,F_j}^{(n)}, \gamma_{F_j,N_i^P}^{(n)})}$$
$$= 2(\alpha_{N_i^P,F_j}^{(n)} - \gamma_{F_j,N_i^P}^{(n)}), \quad (42)$$

$$\frac{\partial f(\alpha_{N_i^P,F_j}, \gamma_{F_j,N_i^P}, \alpha_{N_i^P,F_j}^{(n)}, \gamma_{F_j,N_i^P}^{(n)})}{\partial \gamma_{N_i^P,F_j}}\Big|_{(\alpha_{N_i^P,F_j}^{(n)}, \gamma_{F_j,N_i^P}^{(n)})}$$
$$= \frac{\partial(\alpha_{N_i^P,F_j} - \gamma_{F_j,N_i^P})^2}{\partial \gamma_{N_i^P,F_j}}\Big|_{(\alpha_{N_i^P,F_j}^{(n)}, \gamma_{F_j,N_i^P}^{(n)})}$$
$$= -2(\alpha_{N_i^P,F_j}^{(n)} - \gamma_{F_j,N_i^P}^{(n)}), \quad (43)$$

Based on (40) and (41), we can demonstrate (38) and (39) are satisfied. As a result, Algorithm 1 must converge to the KKT solution of $\mathcal{OP}_1$ [34]. ∎

APPENDIX B
THE PROOF OF THEOREM 2

To prove $\mathcal{OP}_2''$ is a convex optimization problem, we firstly illustrate

$R(\tau_{N_i^T,F_j}, \widetilde{\tau}_{N_i^T,F_j}) = \widetilde{\tau}_{N_i^T,F_j} \log_2(1 + \gamma_{F_j,x_{F_j}}^{(1)'} + \gamma_{F_j,x_{F_j}}^{(2)'})$ is a jointly concave function of both $\tau_{N_i^T,F_j}$ and $\widetilde{\tau}_{N_i^T,F_j}$. For the sake of notational simplicity, let $\Xi_1 = 1 + \gamma_{F_j,x_{F_j}}^{(1)'}$, $\Xi_2 = \frac{\eta |h_{S,N_i^T}|^2 |h_{N_i^T,F_j}|^2}{\frac{\sigma^2}{P_S}}$, i.e., $R(\tau_{N_i^T,F_j}, \widetilde{\tau}_{N_i^T,F_j}) = \widetilde{\tau}_{N_i^T,F_j} \log_2(\Xi_1 + \frac{\tau_{N_i^T,F_j}\Xi_2}{\widetilde{\tau}_{N_i^T,F_j}})$. Obviously, $\log_2(\Xi_1 + \tau_{N_i^T,F_j}\Xi_2)$ is a concave function over $\tau_{N_i^T,F_j}$, and $R(\tau_{N_i^T,F_j}, \widetilde{\tau}_{N_i^T,F_j})$ is the perspective function of $\log_2(\Xi_1 + \tau_{N_i^T,F_j}\Xi_2)$. According to [35], performing a perspective operation on a concave function preserves the nature of concavity. As a result, $R(\tau_{N_i^T,F_j}, \widetilde{\tau}_{N_i^T,F_j})$ is a jointly concave function of w.r.t. $\tau_{N_i^T,F_j}$ and $\widetilde{\tau}_{N_i^T,F_j}$. In the objective function of $\mathcal{OP}_2''$, $R_{N_i^P,F_j}$ is a concave function of $\rho_{N_i^P,F_j}$ and $R_{N_i^T,F_j}$ is a linear function of $\tau_{N_i^T,F_j}$. Thus, the objective function of $\mathcal{OP}_2''$ is concave. Besides, the constraints of $\mathcal{OP}_2''$ restrict the convex sets of the optimization variables. Thus, $\mathcal{OP}_2''$ is a convex optimization problem. ∎

APPENDIX C
THE PROOF OF THEOREM 3

During each iteration in Algorithm 2, two subproblems are performed, i.e., the optimization of power allocation and that of PS and TS control. We denote $\Gamma(\alpha_{N_i^P,F_j}, \alpha_{N_i^T,F_j}, \rho_{N_i^P,F_j}, \tau_{N_i^T,F_j}, \widetilde{\tau}_{N_i^T,F_j})$ as the objective function of the inner resource allocation problem, and $\Gamma(\alpha_{N_i^P,F_j}^{(l)}, \alpha_{N_i^T,F_j}^{(l)}, \rho_{N_i^P,F_j}^{(l)}, \tau_{N_i^T,F_j}^{(l)}, \widetilde{\tau}_{N_i^T,F_j}^{(l)})$ is used to represent the sum-rate calculated at the l-th iteration. In line 4 of Algorithm 2, given $\rho_{N_i^P,F_j}^{(l)}$, $\tau_{N_i^T,F_j}^{(l)}$ and $\widetilde{\tau}_{N_i^T,F_j}^{(l)}$, we have the following inequality

$$\Gamma(\alpha_{N_i^P,F_j}^{(l)}, \alpha_{N_i^T,F_j}^{(l)}, \rho_{N_i^P,F_j}^{(l)}, \tau_{N_i^T,F_j}^{(l)}, \widetilde{\tau}_{N_i^T,F_j}^{(l)})$$
$$\leq \Gamma(\alpha_{N_i^P,F_j}^{(l)}, \alpha_{N_i^T,F_j}^{(l)}, \rho_{N_i^P,F_j}^{(l+1)}, \tau_{N_i^T,F_j}^{(l+1)}, \widetilde{\tau}_{N_i^T,F_j}^{(l+1)}). \quad (44)$$

This is because the resulting values obtained by Algorithm 1 are non-decreasing according to *Theorem 1*. Similarly, in line 5 of Algorithm 2, it is clear to derive

$$\Gamma(\alpha_{N_i^P,F_j}^{(l)}, \alpha_{N_i^T,F_j}^{(l)}, \rho_{N_i^P,F_j}^{(l+1)}, \tau_{N_i^T,F_j}^{(l+1)}, \widetilde{\tau}_{N_i^T,F_j}^{(l+1)})$$
$$\leq \Gamma(\alpha_{N_i^P,F_j}^{(l+1)}, \alpha_{N_i^T,F_j}^{(l+1)}, \rho_{N_i^P,F_j}^{(l+1)}, \tau_{N_i^T,F_j}^{(l+1)}, \widetilde{\tau}_{N_i^T,F_j}^{(l+1)}). \quad (45)$$

Based on (42) and (43), we con conclude the following inequality, i.e., $\Gamma(\alpha_{N_i^P,F_j}^{(l)}, \alpha_{N_i^T,F_j}^{(l)}, \rho_{N_i^P,F_j}^{(l)}, \tau_{N_i^T,F_j}^{(l)}, \widetilde{\tau}_{N_i^T,F_j}^{(l)}) \leq \Gamma(\alpha_{N_i^P,F_j}^{(l+1)}, \alpha_{N_i^T,F_j}^{(l+1)}, \rho_{N_i^P,F_j}^{(l+1)}, \tau_{N_i^T,F_j}^{(l+1)}, \widetilde{\tau}_{N_i^T,F_j}^{(l+1)})$. It is clear that the value of the optimization objective of the inner resource allocation problem is non-decreasing after each iteration. Moreover, the value of the optimization objective is upper bounded by a finite value due to the limited power and time resources in the considered network. As a result, the proposed Algorithm 2 is guaranteed to converge. ∎

REFERENCES

[1] L. Dai, B. Wang, Y. Yuan, S. Han, C. l. I., and Z. Wang, "Non-orthogonal multiple access for 5G: Solutions, challenges, opportunities, and future research trends," *IEEE Commun. Mag.*, vol. 53, no. 9, pp. 74–81, Sep. 2015.

[2] L. Lv, J. Chen, Q. Ni, Z. Ding, and H. Jiang, "Cognitive non-orthogonal multiple access with cooperative relaying: A new wireless frontier for 5G spectrum sharing," *IEEE Commun. Mag.*, vol. 56, no. 4, pp. 188–195, Apr. 2018.

[3] F. Fang, H. Zhang, J. Cheng, S. Roy, and V. C. M. Leung, "Joint user scheduling and power allocation optimization for energy-efficient NOMA systems with imperfect CSI," *IEEE J. Sel. Areas Commun.*, vol. 35, no. 12, pp. 2874–2885, Dec. 2017.

[4] Z. Ding, M. Peng, and H. V. Poor, "Cooperative non-orthogonal multiple access in 5G systems," *IEEE Commun. Lett.*, vol. 19, no. 8, pp. 1462–1465, Aug. 2015.

[5] Z. Shi, W. Gao, S. Zhang, J. Liu, and N. Kato, "AI-enhanced cooperative spectrum sensing for non-orthogonal multiple access," *IEEE Wireless Commun.*, vol. 27, no. 2, pp. 173–179, Apr. 2020.

[6] Z. Shi, W. Gao, S. Zhang, J. Liu, and N. Kato, "Machine learning-enabled cooperative spectrum sensing for non-orthogonal multiple access," *IEEE Trans. Wireless Commun.*, vol. 19, no. 9, pp. 5692–5702, Sep. 2020.

[7] Z. Ning *et al.*, "Mobile edge computing enabled 5G health monitoring for internet of medical things: A decentralized game theoretic approach," *IEEE J. Sel. Areas Commun.*, vol. 39, no. 2, pp. 463–478, Feb. 2021.

[8] M. Wu, Q. Song, L. Guo, and A. Jamalipour, "Charge-then-cooperate: Secure resource allocation for wireless-powered relay networks with wireless energy transfer," *IEEE Trans. Veh. Technol.*, vol. 70, no. 5, pp. 5088–5093, May 2021.

[9] I. Krikidis, S. Timotheou, S. Nikolaou, G. Zheng, D. W. K. Ng, and R. Schober, "Simultaneous wireless information and power transfer in modern communication systems," *IEEE Commun. Mag.*, vol. 52, no. 11, pp. 104–110, Nov. 2014.

[10] P. Ramezani and A. Jamalipour, "Throughput maximization in dual-hop wireless powered communication networks," *IEEE Trans. Veh. Technol.*, vol. 66, no. 10, pp. 9304–9312, Oct. 2017.

[11] S. Kang, H. Lee, S. Jang, H. Kim, and I. Lee, "Dynamic time switching for MIMO wireless information and power transfer," *IEEE Trans. Commun.*, vol. 67, no. 6, pp. 3978–3990, Jun. 2019.

[12] Z. Zhu, S. Huang, Z. Chu, F. Zhou, D. Zhang, and I. Lee, "Robust designs of beamforming and power splitting for distributed antenna systems with wireless energy harvesting," *IEEE Syst. J.*, vol. 13, no. 1, pp. 30–41, Mar. 2019.

[13] Z. Zhu, N. Wang, W. Hao, Z. Wang, and I. Lee, "Robust beamforming designs in secure MIMO SWIPT IoT networks with a nonlinear channel model," *IEEE Internet Things J.*, vol. 8, no. 3, pp. 1702–1715, Feb. 2021.

[14] H. Lee, K. Lee, H. Kim, and I. Lee, "Joint transceiver optimization for MISO SWIPT systems with time switching," *IEEE Trans. Wireless Commun.*, vol. 17, no. 5, pp. 3298–3312, May 2018.

[15] Y. Liu, Z. Ding, M. Elkashlan, and H. V. Poor, "Cooperative nonorthogonal multiple access with simultaneous wireless information and power transfer," *IEEE J. Sel. Areas Commun.*, vol. 34, no. 4, pp. 938–953, Apr. 2016.

[16] Y. Liu, H. Ding, J. Shen, R. Xiao, and H. Yang, "Outage performance analysis for SWIPT-based cooperative non-orthogonal multiple access systems," *IEEE Commun. Lett.*, vol. 23, no. 9, pp. 1501–1505, Sep. 2019.

[17] C. Guo, L. Zhao, C. Feng, Z. Ding, and H. Chen, "Energy harvesting enabled NOMA systems with full-duplex relaying," *IEEE Trans. Veh. Technol.*, vol. 68, no. 7, pp. 7179–7183, Jul. 2019.

[18] N. T. Do, D. B. Da Costa, T. Q. Duong, and B. An, "A BNBF user selection scheme for NOMA-based cooperative relaying systems with SWIPT," *IEEE Commun. Lett.*, vol. 21, no. 3, pp. 664–667, Mar. 2017.

[19] Y. Xu *et al.*, "Joint beamforming and power-splitting control in downlink cooperative SWIPT NOMA systems," *IEEE Trans. Signal Process.*, vol. 65, no. 18, pp. 4874–4886, Sep. 2017.

[20] Y. Yuan, P. Xu, Z. Yang, Z. Ding, and Q. Chen, "Joint robust beamforming and power-splitting ratio design in SWIPT-based cooperative NOMA systems with CSI uncertainty," *IEEE Trans. Veh. Technol.*, vol. 68, no. 3, pp. 2386–2400, Mar. 2019.

[21] B. Su, Q. Ni, and W. Yu, "Robust transmit beamforming for SWIPT-enabled cooperative NOMA with channel uncertainties," *IEEE Trans. Commun.*, vol. 67, no. 6, pp. 4381–4392, Jun. 2019.

[22] J. Liu, K. Xiong, Y. Lu, P. Fan, Z. Zhong, and K. B. Letaief, "SWIPT-enabled full-duplex NOMA networks with full and partial CSI," *IEEE Trans. Green Commun. Netw.*, vol. 4, no. 3, pp. 804–818, Sep. 2020.

[23] Y. Yuan, Y. Xu, Z. Yang, P. Xu, and Z. Ding, "Energy efficiency optimization in full-duplex user-aided cooperative SWIPT NOMA systems," *IEEE Trans. Commun.*, vol. 67, no. 8, pp. 5753–5767, Aug. 2019.

[24] R. Jiang, K. Xiong, P. Fan, Y. Zhang, and Z. Zhong, "Power minimization in SWIPT networks with coexisting power-splitting and time-switching users under nonlinear EH model," *IEEE Internet Things J.*, vol. 6, no. 5, pp. 8853–8869, Oct. 2019.

[25] P. Dinh, M. A. Arfaoui, S. Sharafeddine, C. Assi, and A. Ghrayeb, "A low-complexity framework for joint user pairing and power control for cooperative NOMA in 5G and beyond cellular networks," *IEEE Trans. Commun.*, vol. 68, no. 11, pp. 6737–6749, Nov. 2020.

[26] Z. Ning *et al.*, "Partial computation offloading and adaptive task scheduling for 5G-enabled vehicular networks," *IEEE Trans. Mobile Comput.*, to be published, doi: 10.1109/TMC.2020.3025116.

[27] A. Tolba, "A two-level traffic smoothing method for efficient cloud-IoT communications." *Peer-to-Peer Netw, Appl.*, [Online]. Available: https://doi.org/10.1007/s12083-021-01106-5.

[28] P. Lin, Q. Song, F. R. Yu, D. Wang, and L. Guo, "Task offloading for wireless VR-enabled medical treatment with blockchain security using collective reinforcement learning," *IEEE Internet Things J.*, to be published, doi: 10.1109/JIOT.2021.3051419.

[29] A. Tolba and A. Altameem, "A three-tier architecture for securing IoV communications using vehicular dependencies," *IEEE Access*, vol. 7, pp. 61331–61341, 2019.

[30] W. Peng, W. Gao, and J. Liu, "AI-enabled massive devices multiple access for smart city," *IEEE Internet Things J.*, vol. 6, no. 5, pp. 7623–7634, Oct. 2019.

[31] J. Papandriopoulos and J. S. Evans, "Scale: A low-complexity distributed protocol for spectrum balancing inmultiuser DSL networks," *IEEE Trans. Inf. Theory*, vol. 55, no. 8, pp. 3711–3724, Aug. 2009.

[32] M. Grant, S. Boyd, and Y. Ye, "CVX: Matlab software for disciplined convex programming," 2008.

[33] Y. Mao, B. Clerckx, J. Zhang, V. O. K. Li, and M. A. Arafah, "Max-min fairness of k-user cooperative rate-splitting in MISO broadcast channel with user relaying," *IEEE Trans. Wireless Commun.*, vol. 19, no. 10, pp. 6362–6376, Oct. 2020.

[34] B. R. Marks and G. P. Wright, "A general inner approximation algorithm for nonconvex mathematical programs," *Oper. Res.*, vol. 26, no. 4, pp. 681–683, Jul. 1978.

[35] S. Boyd and L. Vandenberghe, *Convex Optimization*. Cambridge, U.K.: Cambridge Univ. Press, 2004.

[36] X. Wang, Z. Ning, S. Guo, and L. Wang, "Imitation learning enabled task scheduling for online vehicular edge computing," *IEEE Trans. Mobile Comput.*, to be published, doi: 10.1109/TMC.2020.3012509.

[37] H. W. Kuhn and B. Yaw, "The Hungarian method for the assignment problem," *Nav. Res. Logist. Quart*, vol. 2, no. 1, pp. 83–97, Mar. 1955.

[38] X. Lai, Q. Zhang, and J. Qin, "Cooperative NOMA short-packet communications in flat rayleigh fading channels," *IEEE Trans. Veh. Tech.*, vol. 68, no. 6, pp. 6182–6186, Jun. 2019.

[39] W. Liang, Z. Ding, Y. Li, and L. Song, "User pairing for downlink non-orthogonal multiple access networks using matching algorithm," *IEEE Trans. Commun.*, vol. 65, no. 12, pp. 5319–5332, Dec. 2017.
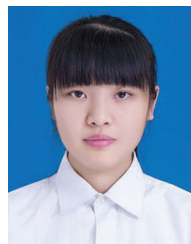
Mengru Wu (Student Member, IEEE) received the M.S. degree in communication and information systems from Northeastern University, Shenyang, China, in 2018, where she is currently working toward the Ph.D. degree in communication and information systems. She is also with the School of Electrical Engineering, Korea University, Seoul, South Korea, as a Visiting Student sponsored by the China Scholarship Council. Her current research interests include wireless power transfer, nonorthogonal multiple access, physical-layer security, mobile edge computing, and resource allocation.

Qingyang Song (Senior Member, IEEE) received the Ph.D. degree in telecommunications engineering from the University of Sydney, Sydney, NSW, Australia, in 2007. From 2007 to 2018, she was with Northeastern University, Shenyang, China. In 2018, she joined the Chongqing University of Post and Telecommunications, Chongqing, China, where she is currently a Professor. She has authored more than 100 papers in major journals and international conferences. Her current research interests include cooperative resource management, edge computing, vehicular ad hoc network, mobile caching, and simultaneous wireless information and power transfer. She is on the Editorial Boards of two publications, the Editor of the IEEE TRANSACTIONS ON VEHICULAR TECHNOLOGY and the Academic Editor of the *Digital Communications and Networks*.

Lei Guo (Member, IEEE) received the Ph.D. degree in communication and information systems from the University of Electronic Science and Technology of China, Chengdu, China, in 2006. He is currently a Full Professor of communication and information systems with the Chongqing University of Posts and Telecommunications, Chongqing, China. He has authored or coauthored more than 200 technical papers in international journals and conferences. His research interests include communication networks, optical communications, and wireless communications. He is the Editor of various international journals.

Abbas Jamalipour (Fellow, IEEE) received the Ph.D. degree in electrical engineering from Nagoya University, Nagoya, Japan. He is currently a Professor of ubiquitous mobile networking with the University of Sydney, Sydney, NSW, Australia. He has authored nine technical books, eleven book chapters, more than 550 technical papers, and five patents, in the area of wireless communications. He was the recipient of the number of prestigious awards, including the 2019 IEEE ComSoc Distinguished Technical Achievement Award in Green Communications, the 2016 IEEE ComSoc Distinguished Technical Achievement Award in Communications Switching and Routing, the 2010 IEEE ComSoc Harold Sobol Award, the 2006 IEEE ComSoc Best Tutorial Paper Award, and 15 Best Paper Awards. He is the President of the IEEE Vehicular Technology Society. He held the positions of the Executive Vice-President and the Editor-in-Chief of VTS Mobile World and has been an elected Member of the Board of Governors of the IEEE Vehicular Technology Society since 2014. He was the Editor-in-Chief of the IEEE WIRELESS COMMUNICATIONS, the Vice President-Conferences, and a Member of Board of Governors of the IEEE Communications Society. He sits on the Editorial Board of the IEEE ACCESS and is the Editor of the IEEE TRANSACTIONS ON VEHICULAR TECHNOLOGY, and various other journals. He has been the General Chair or Technical Program Chair for a number of conferences, including IEEE ICC, GLOBECOM, WCNC, and PIMRC. He is a Fellow of the Institute of Electrical, Information, and Communication Engineers and the Institution of Engineers Australia, an ACM Professional Member, and an IEEE Distinguished Speaker.